

LOW PROFILE DUAL BAND SHARED ANTENNA ARRAY FOR VEHICLE TO VEHICLE COMMUNICATION

Submitted by

THIRUVAZHI DHINESH KUMAR S (2019105594)

GOWTHAM N (2019105532)

DINESH M (2019105526)

KAVIYARASAN K (2019105021)

In partial fulfillment for the award of the degree of

BACHELOR OF ENGINEERING

in

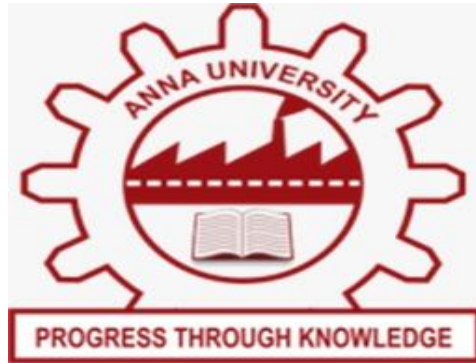
ELECTRONICS AND COMMUNICATION ENGINEERING

COLLEGE OF ENGINEERING, GUINDY

ANNA UNIVERSITY::CHENNAI 600025

MAY 2023

APPENDIX 2



ANNA UNIVERSITY: CHENNAI 600 025

BONAFIDE CERTIFICATE

Certified that this project report **LOW PROFILE DUAL BAND SHARED ANTENNA ARRAY FOR VEHICLE TO VEHICLE COMMUNICATION** is the bonafide, work of **GOWTHAM N** who carried the project work under my supervision.

SIGNATURE

Dr.M.Meenakshi

HEAD OF THE DEPARTMENT

PROFESSOR

DEPARTMENT OF ECE

COLLEGE OF ENGINEERING, GUINDY

ANNA UNIVERSITY

CHENNAI-600 025

SIGNATURE

Dr.M.Shanmugapriya

SUPERVISOR

ASSISTANT PROFESSOR

DEPARTMENT OF ECE

COLLEGE OF ENGINEERING, GUINDY

ANNA UNIVERSITY

CHENNAI-600 025

ACKNOWLEDGEMENT

First and foremost, we thank God for an abundance of grace and has countless blessings in making this work a great success.

We also express our sincere gratitude to our Head of the Department **Dr.M.MEENAKSHI**, Professor, Department of Electronics and Communication Engineering for her enthusiastic encouragement and support throughout the project.

We present our sincere thanks and gratitude to our project supervisor, **Dr.M.SHANMUGAPRIYA**, Assistant Professor, Department of Electronics and Communication Engineering for his wholehearted support, patience, valuable guidance, technical expertise and encouragement in our project.

We thank all the teaching and non-teaching staff of Department of Electronics and Communication Engineering, for their kind help and co-operation during the course of our project.

APPENDIX 3

TABLE OF CONTENTS

Chapter No.	Section No.	Title	Page No.
		Abstract	i
		List of Tables	iii
		List of Figures	iv
1		Introduction	1
	1.1	Motivation	2
	1.2	Software Requirement	3
	1.3	Software Overview	3
2		Literature Survey	4
3		Simulation Design Methodology and Results	
	3.1	Design flow	6
	3.2	CST Procedure	9
	3.3	Analysis I	10
	3.4	Analysis II	15
	3.5	Analysis III	21
	3.6	Analysis IV	28
4		Fabrication Process	
	4.1	Laser cum chemical etching	24
	4.2	Final Preparations	27
	4.3	Laser depaneling	28
	4.4	Network Analyzer	29
	4.5	Calibration kit	30
	4.6	SMA connector	31
5		Fabrication results	
	5.1	Results	33
6		Conclusion	36
		References	37

ABSTRACT

In this project, a dual-band shared aperture antenna array is designed that operates at both the current Dedicated Short Range Communications (DSRC) band (viz. 5.9 GHz) and the future 5G millimeter-wave (mm-wave) band allocated for vehicle-to-vehicle (V2V) communications. The design consists of a 2 x 2 differentially fed patch array operating at 5.9 GHz, co-printed with a 1 x 2 series fed array operating on a single-layer substrate. Two antenna arrays have been designed using two different substrates: Rogers RT Duroid 5880 and FR4, and the effect of substrate material type on antenna performance has been studied. In particular, the shared aperture array designed using Rogers operates from 5.854–6.001 GHz (DSRC band) with a bandwidth of 147 MHz and a gain of 10.63 dB intended for V2V communication. It also operates from 25.626–26.362 GHz (5G mm-wave band) with a bandwidth of 736 MHz and a gain of 9.778 dB intended for 5G mm-wave communication. The ports of the array are highly isolated, with an isolation of greater than 50 dB between the DSRC band port and the 5G mm-wave band port.

சுருக்கம்

இந்த திட்டத்தில், தற்போதைய அர்ப்பணிக்கப்பட்ட குறுகிய தூர தொடர்புகள் (DSRC) பேண்ட் (அதாவது 5.9 GHz) மற்றும் எதிர்கால 5G மில்லிமீட்டர்-அலை (mm-wave) பேண்ட் ஆகிய இரண்டிலும் செயல்படும் இரட்டை-பேண்ட் பகிர்வு துளை ஆண்டெனா வரிசை வடிவமைக்கப்பட்டுள்ளது. -வாகனத்திற்கு (V2V) தொடர்புகள். வடிவமைப்பு 5.9 GHz இல் இயங்கும் 2 x 2 வித்தியாசமாக ஊட்டப்பட்ட பேட்ச் வரிசையைக் கொண்டுள்ளது, ஒரு அடுக்கு அடி மூலக்கூறில் செயல்படும் 1 x 2 தொடர் ஃபெட் வரிசையுடன் இணைந்து அச்சிடப்பட்டது. இரண்டு வெவ்வேறு அடி மூலக்கூறுகளைப் பயன்படுத்தி இரண்டு ஆண்டெனா வரிசைகள் வடிவமைக்கப்பட்டுள்ளன: Rogers RT Duroid 5880 மற்றும் FR4, மேலும் ஆண்டெனா செயல்திறனில் அடி மூலக்கூறு வகையின் விளைவு ஆய்வு செய்யப்பட்டுள்ளது. குறிப்பாக, Rogers ஐப் பயன்படுத்தி வடிவமைக்கப்பட்ட பகிரப்பட்ட துளை வரிசையானது 5.854–6.001 GHz (DSRC பேண்ட்) இலிருந்து 147 MHz அலைவரிசையுடன் இயங்குகிறது மற்றும் V2V தகவல்தொடர்புக்காக 10.63 dB ஆதாயத்துடன் செயல்படுகிறது. இது 25.626–26.362 GHz (5G mm-wave band) இலிருந்து 736 MHz அலைவரிசை மற்றும் 9.778 dB இன் ஆதாயத்துடன் 5G mm-அலைத் தொடர்புக்காக செயல்படுகிறது. DSRC பேண்ட் போர்ட் மற்றும் 5G mm-வேவ் பேண்ட் போர்ட்டுக்கு இடையே 50 dB க்கும் அதிகமான தனிமைப்படுத்தலுடன், வரிசையின் துறைமுகங்கள் மிகவும் தனிமைப்படுத்தப்பட்டுள்ளன.

LIST OF FIGURES

Figure No.	Title	Page No.
1	Antenna design	6
2	Antenna array for DSRC band (CST Simulation)	7
3	Antenna array for 5G mm wave band (CST Simulation)	8
4	Design of combined arrays	9
5	Modified design with truncated corners and cross slots in 5.9 GHz array	10
6	Modified design with truncated corners and cross slots in 5.9 GHz array and cross slots in 5G mm wave band array	10
7	Modified design with cross slots in 5.9 GHz array and 5G mm wave band array	11
8	FR4 design	11
9	Modified FR4 design with truncated corners	12
10	S_{11} plot of design containing only 5.9 GHz array	14
11	S_{22} plot of design containing only 28 GHz array	15
12	VSWR plot of design containing only 5.9 GHz array	15
13	VSWR plot of design containing only 28 GHz array	15
14	S_{11} plot of 5.9 GHz array	17
15	S_{22} plot of 28 GHz array	17
16	VSWR plot for 5.9 GHz array	18
17	VSWR plot for 28 GHz array	18
18	Port 1 (5.9 GHz array) is excited	19
19	Port 2 (28 GHz array) is excited	19
20	Design without 180° Phase shift	19

Figure No.	Title	Page No.
21	Design with 180° Phase shift	19
22	Varying patch length (L_p) of the DSRC band array	22
23	Varying patch width (W_p) of the DSRC band array	22
24	Varying patch length (LU_p) of the 5G band array	23
25	Varying patch width (WU_p) of the 5G band array	23
26	Varying thickness of the substrate EPOCH 1	24
27	Varying thickness of the substrate EPOCH 2	24
28	Varying thickness of the substrate EPOCH 3	24
29	S_{11} Plot after slot introduction	25
30	S_{22} Plot after slot introduction	25
31	. Radiation pattern of shared array at 5.9 GHz – Rogers based design	26
32	Radiation pattern of shared array at 26 GHz – Rogers based design	26
33	VSWR at 5.9 GHz – Rogers based design	27
34	VSWR at 26 GHz – Rogers based design	27
35	Axial ratio at DSRC band– Rogers based design	28
36	Axial ratio at 5G mm-wave band– Rogers based design	28
37	S_{11} Plot for 5.9 GHz array – FR4 based design	29
38	S_{22} Plot for 5G mm-wave band – FR4 based design	29
39	Radiation pattern of shared array at 5.9 GHz – FR4 based design	30
40	Radiation pattern of shared array at 5G mm-wave band – FR4 based design	30
41	VSWR at 5.9 GHz – FR4 based design	31

Figure No.	Title	Page No.
42	VSWR at 5G Band – FR4 based design	31
43	Axial ratio at 5.9 GHz – FR4 based design	31
44	Axial ratio at 5G band – FR4 based design	32
45	RAYCUS LASER	34
46	IPG LASER	34
47	After reaction with FeCl ₃	35
48	During tinning process	36
49	During Grinding process	36
50	LPKF Machine	37
51	Gerber of the array	38
52	Insertion of drills beats	38
53	Etched Substrate	39
54	Soldered ports	39
55	Vector Network Analyzer	40
56	Calkit 85220A	40
57	SMA Connector	41
58	Measured S ₁₁ of DSRC band	42
59	Measured VSWR at DSRC band	43

LIST OF TABLES

Table No.	Title	Page No.
1	Dimensions for 5.9 GHz array	7
2	Dimensions for 5G mm-wave band antenna array	8
3	Dimensions for Antenna design using FR4 substrate	12
4	Dimensions for Antenna design using FR4 substrate with truncated corners	13
5	Radiation plots of individual antenna arrays	16
6	Radiation plots for combined array antenna design	18
7	Results without 180° Phase shift – 5.9 GHz array	20
8	Results with 180° Phase shift – 5.9 GHz array	20
9	Results without 180° Phase shift – 28 GHz array	20
10	Results with 180° Phase shift – 28 GHz array	20
11	Simulation results for 5.9 GHz array - Rogers based design	26
12	Simulation results for 26 GHz array - Rogers based design	26
13	Simulation results for 5.9 GHz array – FR4 based design	30
14	Simulation results for 5G mm-wave band – FR4 based design	30

CHAPTER 1

INTRODUCTION

1.1 MOTIVATION:

Globally, road accidents claim 1.3 billion lives per year. Particularly in the US, road accidents result in 38 thousand deaths per year. Improving the safety of the drivers is one of the primary goals of the intelligent transportation system. The Federal Communications Commission (FCC) allocated the 5.85-5.925GHz Dedicated Short Range Communications (DSRC) band in the intelligent transport system (ITS) radio for vehicular communications. This enabled the development of a virtual traffic light (VTL) algorithm to reduce traffic congestion using vehicle-to-vehicle communication (V2V) and internet of things (IoT) technologies. The role of the algorithm is to collect data such as speed, acceleration, and direction of the vehicle from nearby vehicles as well as to control traffic without using physical traffic lights. Field trials conducted in Pittsburgh showed that VTL can effectively reduce 1) road accidents at the intersections by 70%, 2) carbon emissions, and 3) commute time from 30.7 to 18.3 minutes. Currently, the US Department of Transportation and various automobile industries use the 5.9 GHz safety band for automatic toll collection, traffic congestion control, emergency vehicle warning, and intersection movement warning. However, due to bandwidth restriction in the DSRC band, high data rate communications, such as video streaming, are quite difficult to achieve. Therefore, the trend is to move towards the millimeter-wave (mm-wave) spectrum for higher speed communications of >1 Gbps with wider bandwidth and reduced interference. In addition, the radios at mm-wave are smaller in size and require low power consumption, implying inconspicuous integration on the vehicular platforms. However, mm-wave spectrum suffers from large propagation and atmospheric losses as well as attenuation due to rain and severe weather conditions. These losses can be compensated by using high gain antenna arrays. Importantly, we need a system capable of switching between the 5G mm-wave band, for high speed communications, and well-established the DSRC band to meet the required communication link quality of service during severe weather conditions.

Radios that can operate in the traditional low frequency bands and the new mm-wave bands are called non-standalone devices. The main challenge is implementing these devices in a single compact package when the two frequency bands are widely separate with a band ratio $>2:1$. These dual-band systems offer high jamming, and interference protection, as well as improvement in the channel capacity by making use of frequency diversity. Traditionally, dual-band radios employ antennas designed using two separate single-band antennas or a single structure that resonates at both bands. Various works have been reported of multi-band antennas using a single feed. However, these single feed dual-band antennas require additional RF components in the front-end for separate multiband operation. A more efficient design for multiband operation is to use separate feed network for each operating frequency bands by adopting a single or multilayer design. The main drawback of multilayer designs are the multilayer fabrication technique that is expensive and increases the size of the array. One of the simple, and easy fabrication technique is using a single layer Printed Circuit Board (PCB). The implemented PCB shared aperture array operates at dual band with highly isolated ports and provides gain improvement at upper band by utilizing the higher order modes of the lower band array. In this work, a low profile non-standalone, dual-band, shared aperture antenna array with gain improvement is designed for V2V communication. The designed array consists of 4 patch antennas operating at 5.9 GHz (DSRC) with a differential coax feed network and 2 patch antennas operating at 28 GHz (5G mm-wave) with a series coax feed network, as shown. The array provides a dual-band operation with high gain, high port-to-port isolation, and high efficiency.

1.2 SOFTWARE REQUIREMENT:

CST STUDIO SUITE

1.3 SOFTWARE OVERVIEW:

The designs and simulations in this project are based on the Computer Simulation Technology (CST) microwave Studio suite which is a high performance electromagnetic simulation software. There are two basic solver modules provided: time domain solver and frequency domain solver. The two solvers are totally different. Time domain solver is used for non-resonant structures and frequency domain solver contains alternatives for highly

resonant structures. Beside frequency domain solver has the option of utilizing tetrahedral mesh that can discretize the structure better which is not available with in time domain solver. In addition, time domain solver is only for normal incidence but frequency domain solver can be used for off-normal incidences. CST contains several different simulation methods, including the finite integration technique(FIT), finite element method (FEM), transmission line matrix (TLM), multilevel fast multiples method (MLFMM) and particle in cell (PIC), as well as Multiphysics solvers for other domains of physics with links to electromagnetics.

CHAPTER 2

LITERATURE SURVEY

2.1.1 Low Profile Dual-Band Shared Aperture Array for Vehicle-to-Vehicle Communication

In this paper, it was observed that a non-standalone dual-band shared aperture antenna array can be operated at both the current Dedicated Short-Range Communications (DSRC) band (viz. 5.9 GHz) and the future 5G millimeter-wave (mm-wave) band (viz. 28 GHz) allocated for vehicle-to-vehicle (V2V) communications.

2.1.2 Left-Handed Circularly Polarized Two-Element Antenna Array for Vehicular Communication

From this paper, it was observed that truncated opposite corners and introduction of cross slots move the polarization of an antenna from linear towards circular and cause narrow beam width.

2.1.3 Vehicle Platform Effects on Performance of Flexible, Lightweight, and Dual-Band Antenna for Vehicular Communications

From this paper, the impact of the ground, of the vehicle surroundings and of the car body on signal transmission and reception of a dual-band microwave antenna tested on two automotive plastic parts on a convertible vehicle for cellular and Cellular - Vehicle to Everything (C-V2X) communications was observed.

2.1.4 Combined LTE and IEEE 802.11p Antenna for Vehicular Applications

From this paper, the evolution of IEEE 802.11 to IEEE 802.11p with added V2V and V2X technologies which focuses on traffic safety and traffic efficiency has been observed. The observed results show that the antennas are well matched and well isolated for both LTE and V2X.

2.1.5 A Hybrid-Equivalent Surface-Edge Current Model for Simulation of V2X Communication Antennas with Arbitrarily Shaped Contour

From this paper, it was observed that equivalent models of antennas are useful for the fast simulation of vehicle-to-everything (V2X) communication. However, the full-wave methods are accurate but computationally intensive, and they need a supercomputing platform to simulate V2X communication.

2.1.6 A Pillbox Based Dual Circularly-Polarized Millimeter-Wave Multi-Beam Antenna for Future Vehicular Radar Applications

From this paper, it was observed that a series-fed microstrip line based dual CP leaky-wave antenna (LWA) array, which has a symmetrical structure can be used to obtain both left-hand circular polarization (LHCP) and right-hand circular polarization (RHCP) by switching the exciting current direction of the microstrip line.

2.1.7 A dual band omni-directional antenna for WAVE and Wi-Fi

From this paper, it was observed that a dual band antenna is capable of operating in both the WAVE and Wi-Fi bands. This antenna is observed to be simple, easy-to-produce and inexpensive; it can be a cost-effective alternative to use of multiple directional antennas for vehicles.

2.1.8 A Miniaturized Wideband Antenna for Vehicular Communication, WiMAX, and WLAN Applications

From this paper, it was observed that Rogers RT/Duroid 5880 TM with dielectric constant 2.2 and loss tangent $\tan \delta = 0.0009$ has lower loss, higher efficiency and wider bandwidths can be achieved. And also, with an increase in permittivity, the capacitance increases. With an increase in capacitance, the resonant frequency decreases.

CHAPTER 3

SIMULATION DESIGN METHODOLOGY AND RESULTS

3.1 DESIGN FLOW:

3.1.1 Design flow using Rogers substrate:

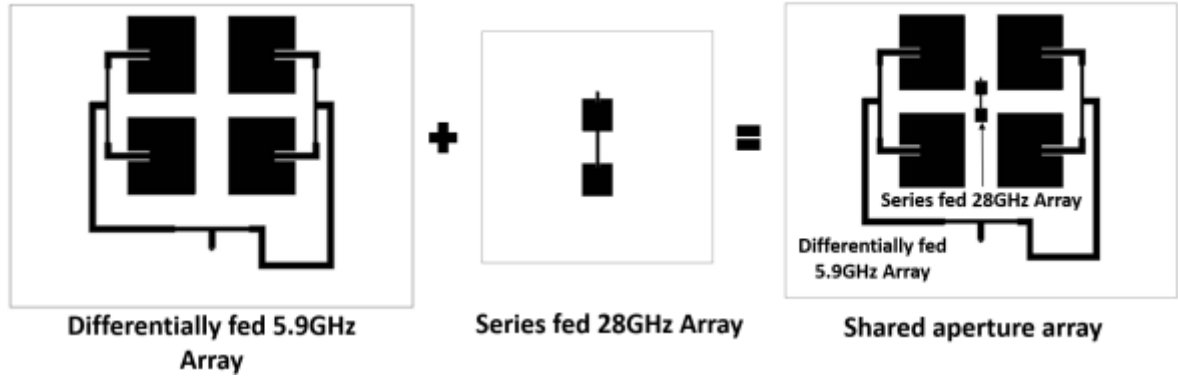


Figure 1. Antenna design

The proposed antenna structure as per the base reference paper consists of two main parts, as shown in Figure. 1, the first part 5.9GHz differential fed array and the second part is series fed 5G mm wave array. Each of the array and coaxially fed and printed upon Rogers substrate. A 28GHz array has been inserted in a space between the 5.9GHz array for future 5G mm wave communication.

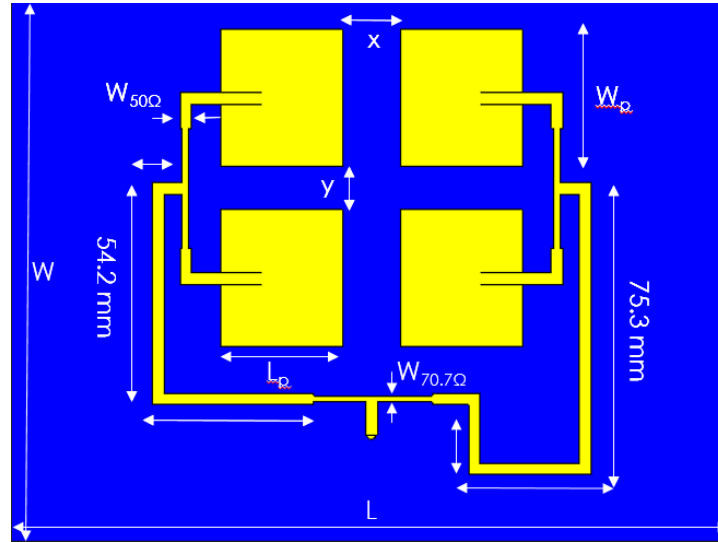


Figure 2. Antenna array for DSRC band (CST Simulation)

Table 1: Dimensions for 5.9 GHz array

PARAMETERS	VALUES(mm)
$W \times L \times h$	$75 \times 100 \times 0.52$
$W_p \times L_p \times h_p$	$19 \times 16.7 \times 0.035$
x	8
y	6
$W_f \times L_{fi} \times h_f$	$1.6 \times 5.85 \times 0.035$
$W_{50\Omega}$	1.6
$W_{70.7\Omega}$	0.9
W_{gap}	0.16

Initially, the antenna array design for 5.9 GHz has been completed as in Figure 2 with differential feeding and simulated to observe the results without presence of a second port in order to compare the results obtained with presence of another port for 5G mm wave band which provides information about the isolation between the ports. Then, another new antenna array for 5G mm wave band has been completed as in Figure 3 with serial feeding and similarly simulation has been done to observe the results without presence of first port which was used for 5.9 GHz.

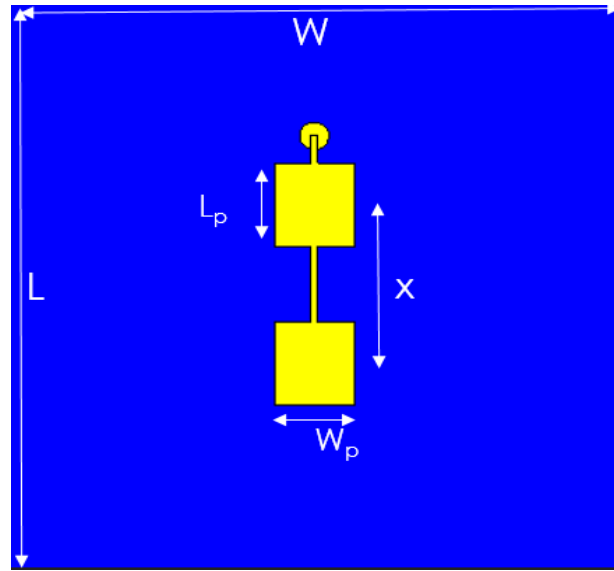


Figure 3. Antenna array for 5G mm wave band (CST Simulation)

Table 2: Dimensions for 5G mm wave band antenna array

PARAMETERS	VALUES(mm)
$W \times L \times h$	$25 \times 25 \times 0.52$
$W_p \times L_p \times h_p$	$3.25 \times 3.67 \times 0.035$
x	8
$W_f \times L_{fi} \times h_f$	$0.3 \times 1.24 \times 0.035$

After obtaining the results of separate antenna arrays from simulation, both these arrays are mounted on a Rogers substrate material to obtain the results with presence of both ports – Port 1 and Port 2 which are used for exciting 5.9 GHz and 5G mm wave frequency band. In the combined design, 5.9 GHz array is fed using differential feeding and 5G mm wave band array is fed using serial feeding so that the latter can be placed in the space available within the former and the dimensions of both these arrays are same as of the individual array antennas. The antenna array design for combined applications of DSRC band and 5G mm wave band has been completed as in Figure 4 and the results obtained is discussed in section 3.3 .

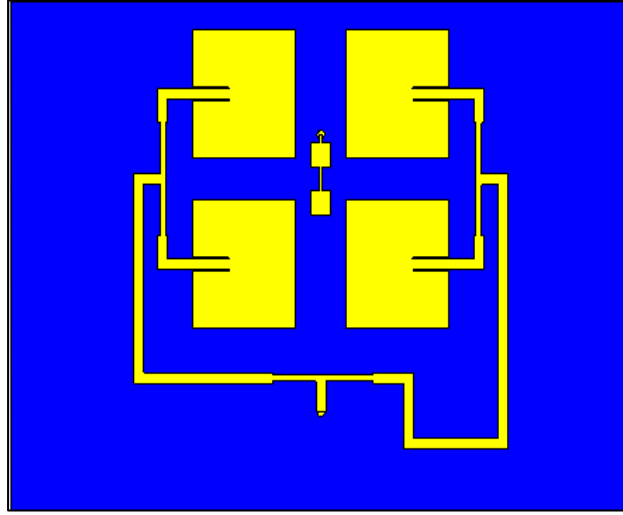


Figure 4. Design of combined arrays

Using the design shown in Figure 4, the resonant frequencies obtained were 5.97 GHz and 28 GHz. For V2V communication the resonant frequency should be 5.9 GHz. In India for 5G, 26 GHz is in use. So to shift the frequencies to left, slots were introduced and the corners of each patch are truncated as shown in Figure 5. Introduction of cross slots, brings forth the advantage of replacing a single radiating element with three radiating elements in place. Increasing the radiating elements with small distance of separation between the elements will narrow down the radiation and increase directivity along with gain. Introducing truncated corners in the regions of the patch where surface current is minimum enhances the performance of the antenna and moves the polarization type of the antenna from linear to circular polarization. Considering these advantages, modifications in the design has been performed through series of parameter sweeps and analysis of surface current distribution. With the design shown in Figure 4, three different modified arrays have been designed as shown in the following figures.

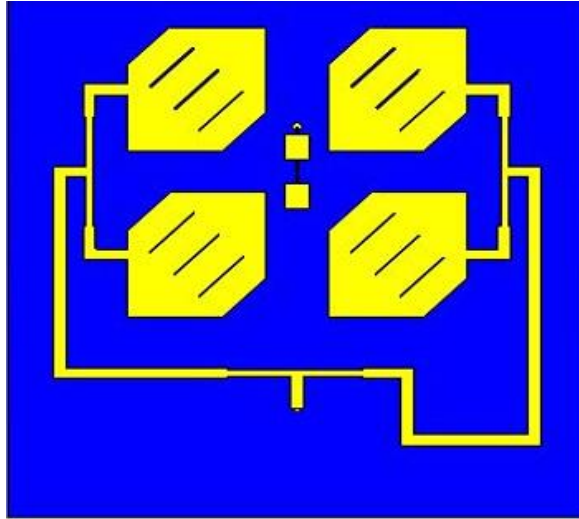


Figure 5. Modified design with truncated corners and cross slots in 5.9 GHz array

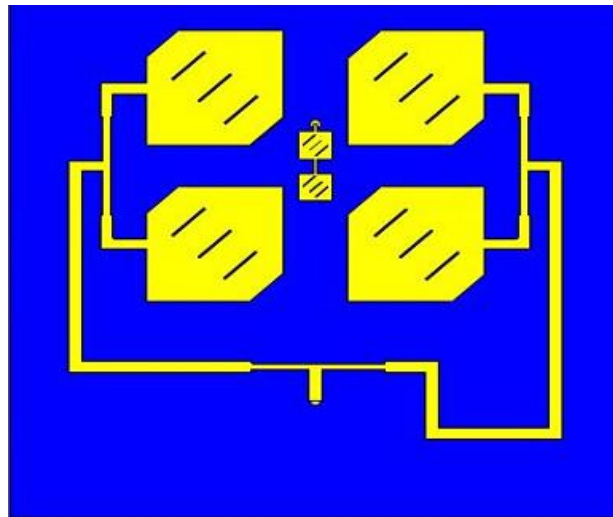


Figure 6. Modified design with truncated corners and cross slots in 5.9 GHz array and cross slots in 5G mm wave band array

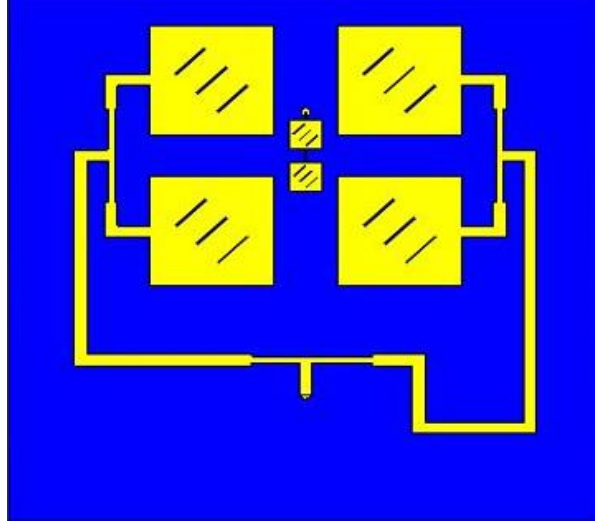


Figure 7. Modified design with cross slots in 5.9 GHz array and 5G mm wave band array

3.1.1 Design flow using FR4 substrate:

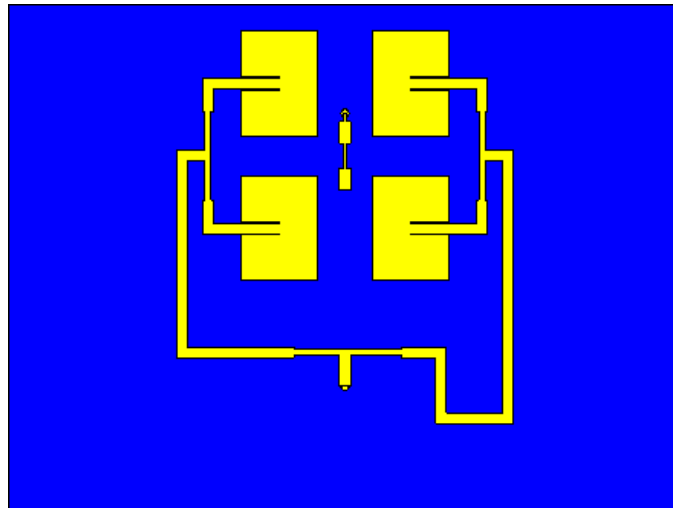


Figure 8. FR4 design

Previous designs were made on substrate based on Rogers. Rogers can be used in any environment. But in V2V communication FR4 can also be used, since the environment does not cause a major impact on the performance of the antenna. Using FR4, the antenna can be made with low cost without degradation in performance. Theoretical calculations have been performed with respect to FR4 substrate and the length and width of the patch of DSRC band array and 5G mm wave band array have been determined and the design has been modified accordingly. The modified dimensions are displayed in Table 3.

Table 3: Dimensions for Antenna design using FR4 substrate

PARAMETERS	VALUES(mm)
$W \times L \times h$	75 x 100 x 0.52
$W_p \times L_p \times h_p$	11.53 x 15.47 x 0.035
x	8
y	6
$W_f \times L_{fi} \times h_f$	1.6 x 5.85 x 0.035
$W_{50\Omega}$	1.6
$W_{70.7\Omega}$	0.9
W_{gap}	0.16
$W_u \times L_u \times h_u$	1.66 x 3.26 x 0.035
X_u	7
$W_f \times L_{fi} \times h_f$	0.3 x 1.24 x 0.035

Introduction of slots in arrays mounted FR4 substrate led to very low resonant frequencies compared to the desired ones. So owing to the advantages in introduction of truncated corners, the FR4 design has been modified with introduction of truncated corners in the patch and the corresponding design is depicted in Figure 9 and the dimension values are displayed in Table 4.

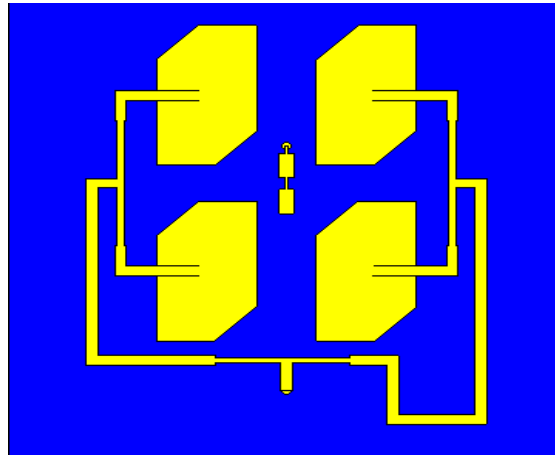


Figure 9. Modified FR4 design with truncated corners

The results obtained using this antenna are discussed in section NN. The design shown in Figure 9 is used for fabrication process and the fabricated antenna is analyzed in section NN.

Table 4: Dimensions for Antenna design using FR4 substrate with truncated corners

PARAMETERS	VALUES(mm)
$W \times L \times h$	$75 \times 75 \times 1.67$
$W_p \times L_p \times h_p$	$23 \times 13.5 \times 0.035$
x	8
y	6
$W_f \times L_{fi} \times h_f$	$1.6 \times 5.85 \times 0.035$
$W_{50\Omega}$	1.6
$W_{70.7\Omega}$	0.9
W_{gap}	0.16
$W_u \times L_u \times h_u$	$2 \times 4 \times 0.035$
X_u	7
$W_f \times L_{fi} \times h_f$	$0.3 \times 1.2 \times 0.035$

3.2 CST PROCEDURE:

Create Ground surface by using a new brick and set the copper as material. Set the dimensions length, width in y length and x length and set 0.035 as height in z length.

Design a substrate with the same length and width as that of the ground component. Set the height starting from z_{max} of ground plane and set z_{max} of the substrate to have the derived height value. Set the material for the substrate to be Rogers.

Now to design the patch on top of the substrate, use new block with copper material

and use the lengths and widths specified in table TT. Design of each patch in antenna array is made using a new block. The feed lines for each element are designed using the parametric values derived and depicted in table TT. To introduce slots on the patches make new blocks with the dimensions of the slots and use boolean operation to cut the patch. Same is to be followed for introducing truncated corners. The translate option is used to rotate the slots and the truncated corner by specifying appropriate angles.

This sequence of steps are carefully followed to get the desired design of the antenna. The parameters for each brick should be given a variable so that the parameter sweeps can be performed easily. A SMA (Sub Miniature version A) connector is used to provide supply. The SMA connector is semi precision coaxial RF connectors developed as a minimal connector interface for coaxial cable with a screw-type coupling mechanism. The results will be varied when SMA connector is used due to noise and the load impedances. The cylinder block is to be made use of, to design the SMA connector. The inner cylinder should have a radius of 0.6 mm and material of Copper. The middle cylinder should have a inner radius of 0.6 mm and outer radius of 1.4 mm and material should be Teflon. The outer cylinder should have a inner radius of 1.4 mm and outer radius of 2.2 mm and the material should be Copper. The outer cylinder should touch the ground plane. The inner cylinder should touch the port of the array of patches to excite the array. Using the steps mentioned two SMA connectors are to be designed for two port – one for 5.9 GHz array and the other for 5G array.

3.3 ANALYSIS I:

The antenna design containing only 5.9 GHz array shown in Figure 2 is excited first. Then the antenna design containing only 28 GHz array shown in Figure 3 is excited.

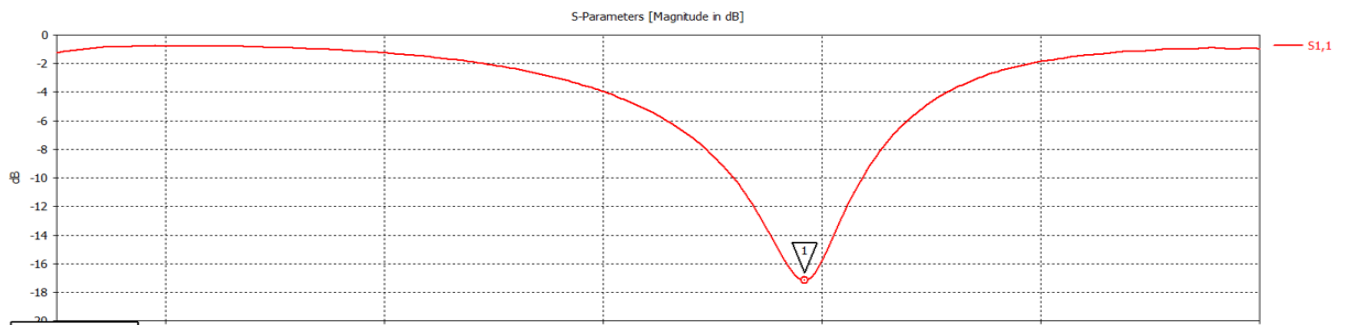


Figure 10. S11 plot of design containing only 5.9 GHz array

The S_{11} and VSWR plots for both the cases are depicted below.

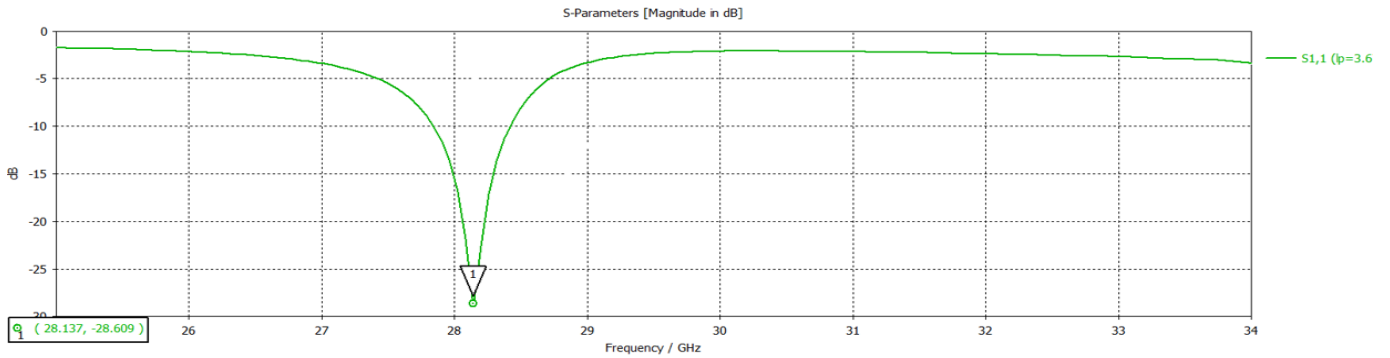


Figure 11. S_{22} plot of design containing only 28 GHz array

The S_{11} plot shows how return loss occur at the resonant frequencies. The desired level of return loss at resonant frequencies is that it should be less than or equal to -10dB. For 5.9 GHz array, S_{11} obtained at 5.98 GHz is about -18dB. For 28 GHz array, the S_{11} obtained at 28.13 GHz is about -30dB.

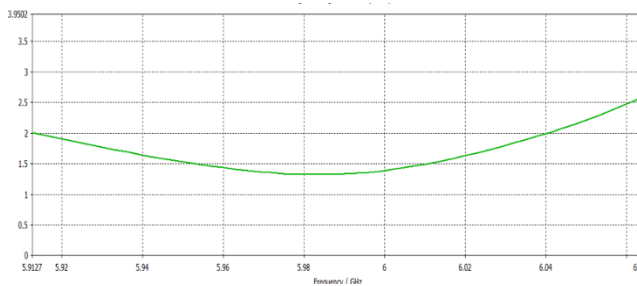


Figure 12. VSWR plot of design containing only 5.9 GHz array

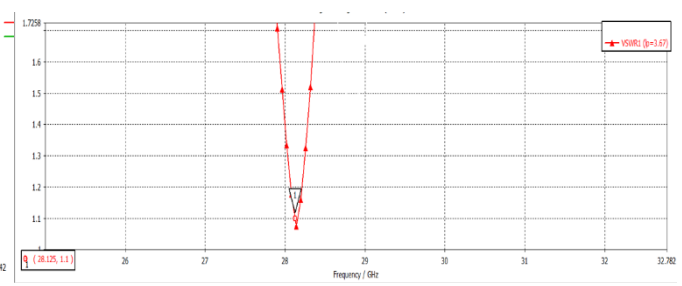
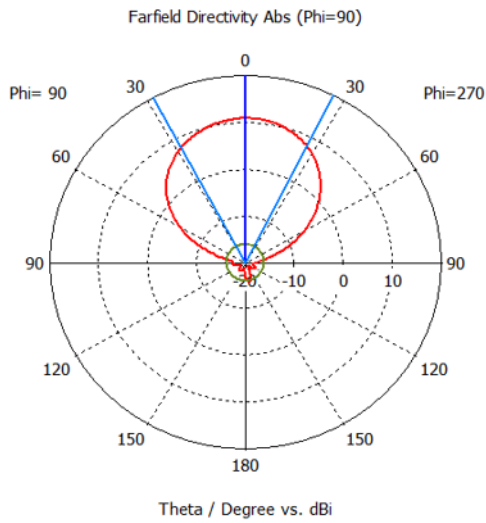


Figure 13. VSWR plot of design containing only 28 GHz array

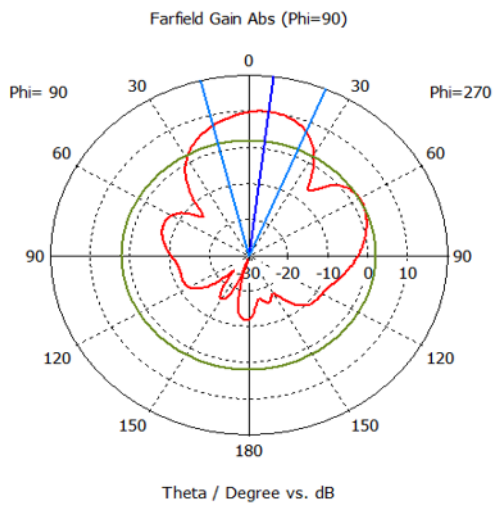
The VSWR which tells about the reflecting wave coefficient should be in the range between 1 and 3 for industrial use. For 5.9 GHz array the VSWR obtained the is near 1.3 and for 28 GHz array VSWR obtained is near 1.09. The individual patch elements are designed to radiate at the desired resonant frequencies. The effect of array can be seen in the radiation pattern, in efficiency, directivity and gain. The radiation pattern obtained by exciting the antenna designs shown in Figure 2 and Figure 3 are depicted in Table 5.

Table 5: Radiation plots of individual antenna arrays



Radiation pattern of 5.9 GHz array

Parameter	Value	
	Single element	2 x 2 array
Gain	5.54 dB	9.99 dB
Directivity	6.478 dB	10.9 dB
Efficiency	80.647 %	79 %
HPBW	91°	55.1°
VSWR	1.1	1.465



Radiation pattern of 28 GHz array

Parameter	Value	
	Single element	1 x 2 array
Gain	6.11 dB	10.2 dB
Directivity	7.77 dB	10.4 dB
Efficiency	68.25 %	94.7 %
HPBW	72.4°	36.8°
VSWR	1.55	1.074

For 5.9 GHz and 28 GHz, when switching from an individual element to an array, gain and directivity have increased and VSWR has decreased. The analysis made by mounting both the array on a single Rogers substrate is discussed below.

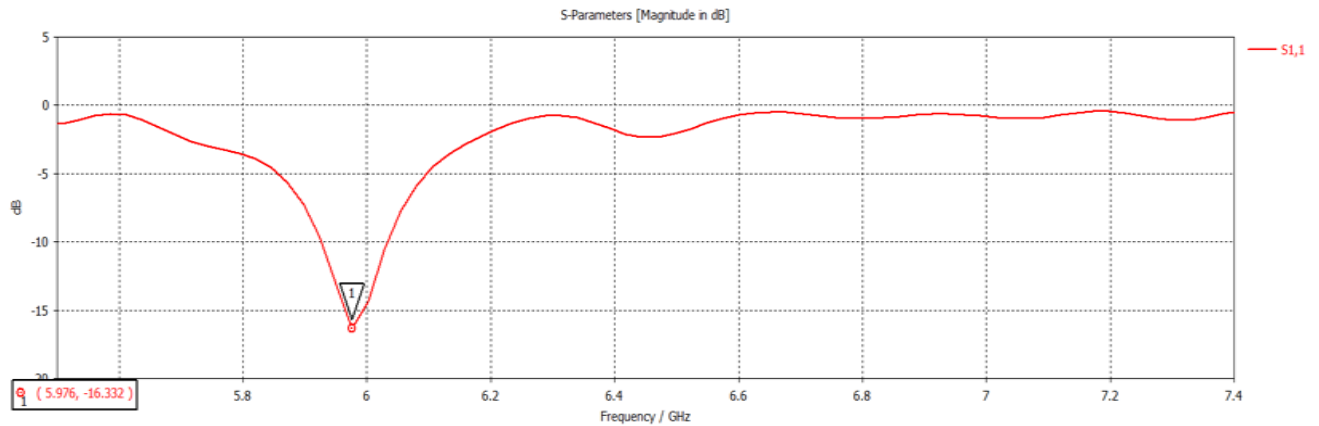


Figure 14. S11 plot of 5.9 GHz array

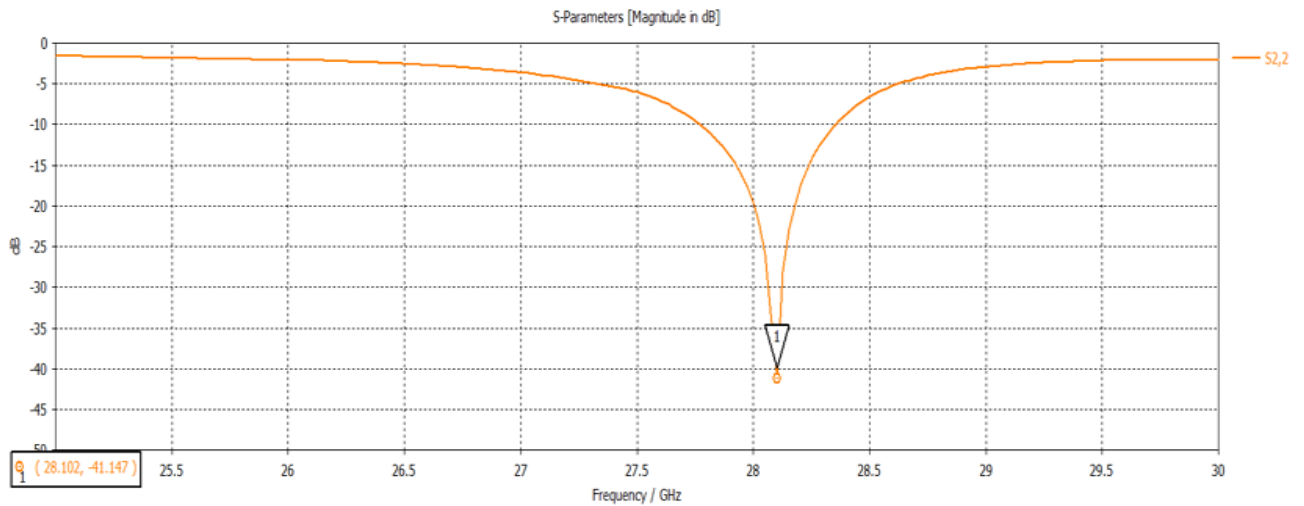


Figure 15. S22 plot of 28 GHz array

The S11 and S22 plots are obtained by exciting the ports of each array on the antenna design shown in figure 4. S11 obtained at 5.976 GHz is about -17dB and S22 obtained at 28.1 GHz is about -41dB. Both S11 and S22 values are good, indicating most of the power fed is radiated.

The VSWR plots are depicted in Figure 16 and 17. VSWR obtained for 5.9GHz is about 1.3 and for 28GHz is 1. This indicates that the reflected wave is very minimum preferable for industrial use.

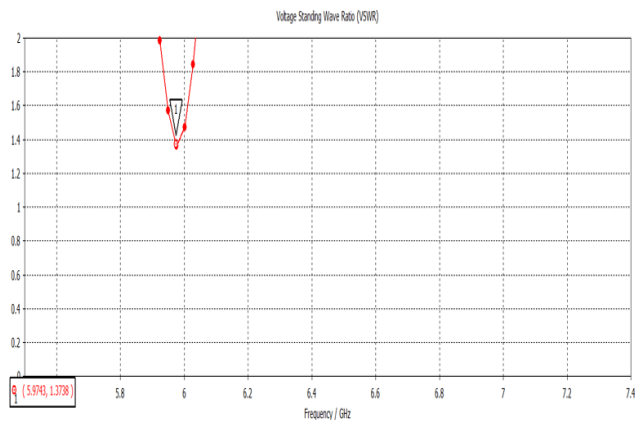


Figure 16. VSWR plot for 5.9 GHz array

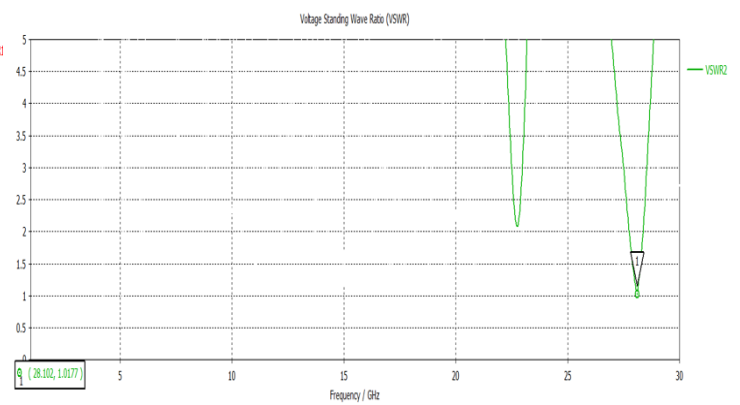


Figure 17. VSWR plot for 28 GHz array

Table 6. Radiation plots of combined array antenna design

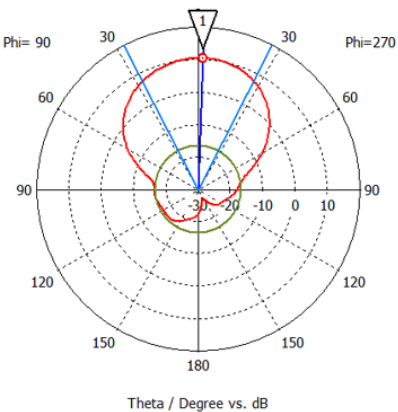
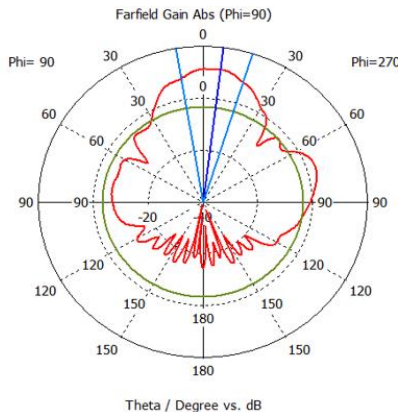
 <p>Radiation pattern for 5.9 GHz array</p>	<table border="1"> <thead> <tr> <th>Parameter</th><th>Value</th></tr> </thead> <tbody> <tr> <td>Gain</td><td>10.5 dB</td></tr> <tr> <td>Directivity</td><td>11.1 dB</td></tr> <tr> <td>Efficiency</td><td>86.6%</td></tr> <tr> <td>HPBW</td><td>54.5°</td></tr> <tr> <td>VSWR</td><td>1.36</td></tr> </tbody> </table>	Parameter	Value	Gain	10.5 dB	Directivity	11.1 dB	Efficiency	86.6%	HPBW	54.5°	VSWR	1.36
Parameter	Value												
Gain	10.5 dB												
Directivity	11.1 dB												
Efficiency	86.6%												
HPBW	54.5°												
VSWR	1.36												
 <p>Radiation pattern for 28 GHz array</p>	<table border="1"> <thead> <tr> <th>Parameter</th><th>Value</th></tr> </thead> <tbody> <tr> <td>Gain</td><td>11.3 dB</td></tr> <tr> <td>Directivity</td><td>11.6 dB</td></tr> <tr> <td>Efficiency</td><td>93.41%</td></tr> <tr> <td>HPBW</td><td>26.8°</td></tr> <tr> <td>VSWR</td><td>1.02</td></tr> </tbody> </table>	Parameter	Value	Gain	11.3 dB	Directivity	11.6 dB	Efficiency	93.41%	HPBW	26.8°	VSWR	1.02
Parameter	Value												
Gain	11.3 dB												
Directivity	11.6 dB												
Efficiency	93.41%												
HPBW	26.8°												
VSWR	1.02												

Table 6 shows the radiation patterns obtained by exciting the ports individually in the combined array design shown in Figure 4. When both the arrays are mounted on the single substrate, minor lobes are introduced in the radiation. To reduce the minor lobes and Half Power Beam Width to increase the directivity, slots are introduced. The analysis done for the antenna design after slots and the truncated corner are introduced, is discussed in section 3.5.

Isolation between the ports is observed in Figure18 and Figure19. The ports are excited individually and observed that power fed to one port is not transferred to the other port.

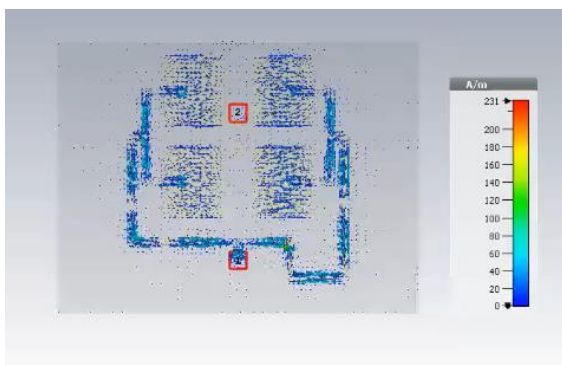


Figure 18. Port 1 (5.9 GHz array) is excited

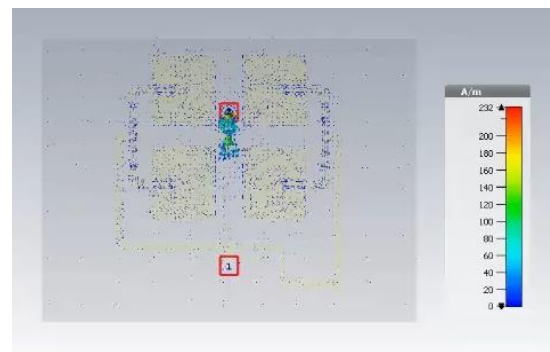


Figure 19. Port 2 (28 GHz array) is excited

3.4 ANALYSIS II: SIGNIFICANCE OF 180° PHASE SHIFT:

DESIGN VARIATIONS:

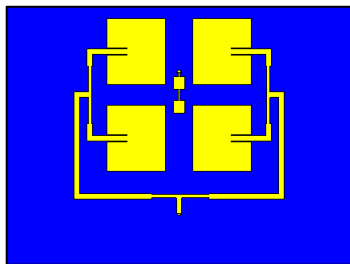


Figure 20. Design without 180° Phase shift

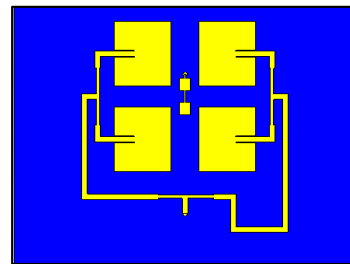


Figure 21. Design with 180° Phase shift

In this antenna, to match the impedance between feed and patch elements, a Quarter wavelength transformer is used. In this transformer, a line having length of one fourth of operating wavelength and characteristic impedance of square root times of characteristic impedance of feed line, is used to connect feed with patch elements.

By controlling the phase difference between powers fed to each element of an antenna array, the radiation pattern can be controlled.

180° out of phase signals when fed to the elements, the lobes can be combined to form a single major lobe.

In 5.9 GHz array, the signal fed to the left 2 elements is 180 degree out of phase with the signal fed to the right 2 elements. This is facilitated by the extended line having length of half of the operating wavelength connected to the right portion of the array. The effect can be observed in the radiation patterns

5.9 GHz RESULTS VARIATION:

Table 7. Results without 180° Phase shift – 5.9 GHz array

Parameter	Value
Gain	8.96 dB
Directivity	9.34 dB
Efficiency	89.7%

Table 8. Results with 180° Phase shift – 5.9 GHz array

Parameter	Value
Gain	10.5 dB
Directivity	11.1 dB
Efficiency	86.6%

28 GHz RESULTS VARIATION:

Table 9. Results without 180° Phase shift – 28 GHz array

Parameter	Value
Gain	8.15 dB
Directivity	9.24 dB
Efficiency	77.8%

Table 10. Results with 180° Phase shift – 28 GHz array

Parameter	Value
Gain	11.3 dB
Directivity	11.6 dB
Efficiency	93.4%

3.5 ANALYSIS III:

MODIFIED ROGERS DESIGN SIMULATION RESULTS

The Rogers design described in the previous section (Schematic can be seen in the figure) is modified by the introduction of cross slots in both DSRC band array and 5G band array referring to the IEEE paper **Left-Handed Circularly Polarized Two-Element Antenna Array for Vehicular Communication** briefly known as **LHCP**. This modified

Rogers design is shown in the figure. After this modification, the corresponding simulation results have been studied.

Compared to the conventional rectangular patch antenna, slot loading antennas give the better performance in

- Resonant frequency,
- High return loss,
- Wider bandwidths etc.

Though the introduction of cross slots brings better efficiency and directivity etc. in the antenna, it is necessary to bring the resonant frequencies to the required place (i.e., DSRC band and 5G band). Thus, it becomes indispensable to do parameter sweeps to bring the resonant frequencies to the desired place.

Shift in the resonance frequency to left or right side while designing the micro-strip patch antenna can be done in many ways.

Two methods in their most basic form are:

- a) By changing the length (dimension) of the patch.
- b) By changing the dielectric constant of the substrate.

Moreover, there are also some other techniques to reduce the resonance frequency of the patch antenna, such as DGS, Metamaterial etc. Apart from this, ABS cover over the patch (used generally to protect against weather) creates effect to move frequency towards left (decrease in resonance frequency).

As the first case, it was attempted to change the dimension (length and width) of the array patch in both DSRC band and 5G band.

The following changes have been done and the parameter sweeps have been conducted:

- Varying patch length of the DSRC band array
- Varying patch width of the DSRC band array

- Varying patch length of the 5G band array
- Varying patch width of the 5G band array
- Varying thickness of the substrate

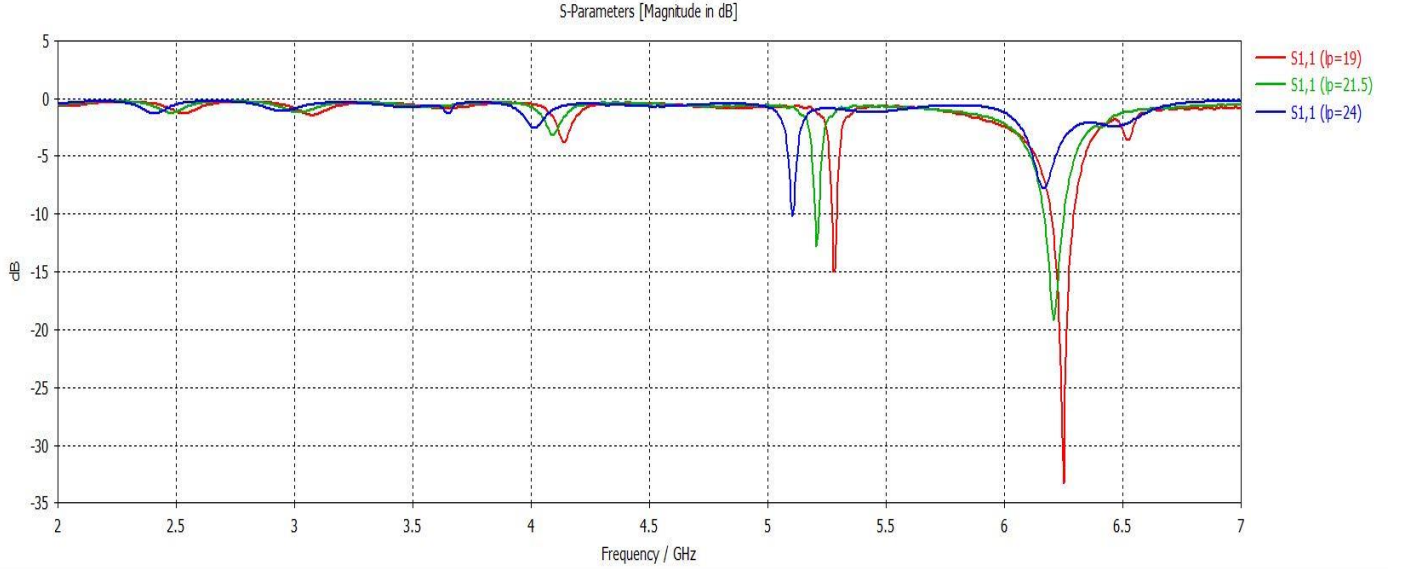


Figure 22. Varying patch length (L_p) of the DSRC band array

From the above figure, it can be inferred that when the length of the patch is increased, the resonant frequency shifts towards left (decrease in the resonant frequency) and vice versa.

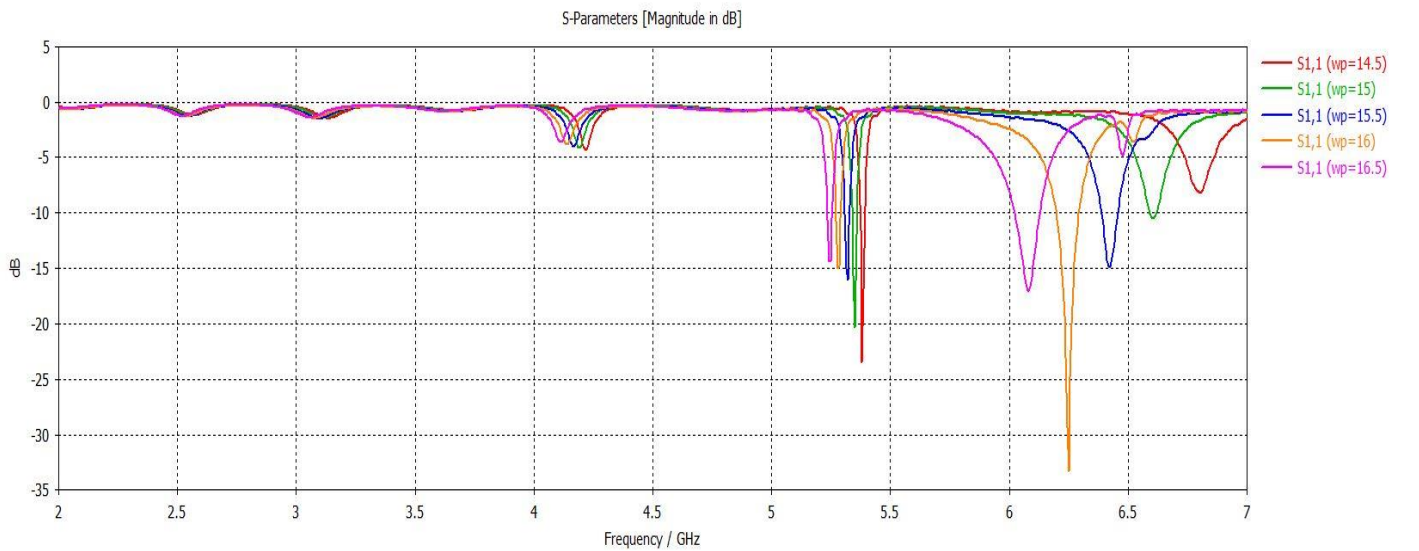


Figure 23. Varying patch width (W_p) of the DSRC band array

From the above figure, it can be inferred that when the width of the patch is increased, the resonant frequency is shifted towards left (i.e., there is a decrease in the resonant frequency) and vice versa.

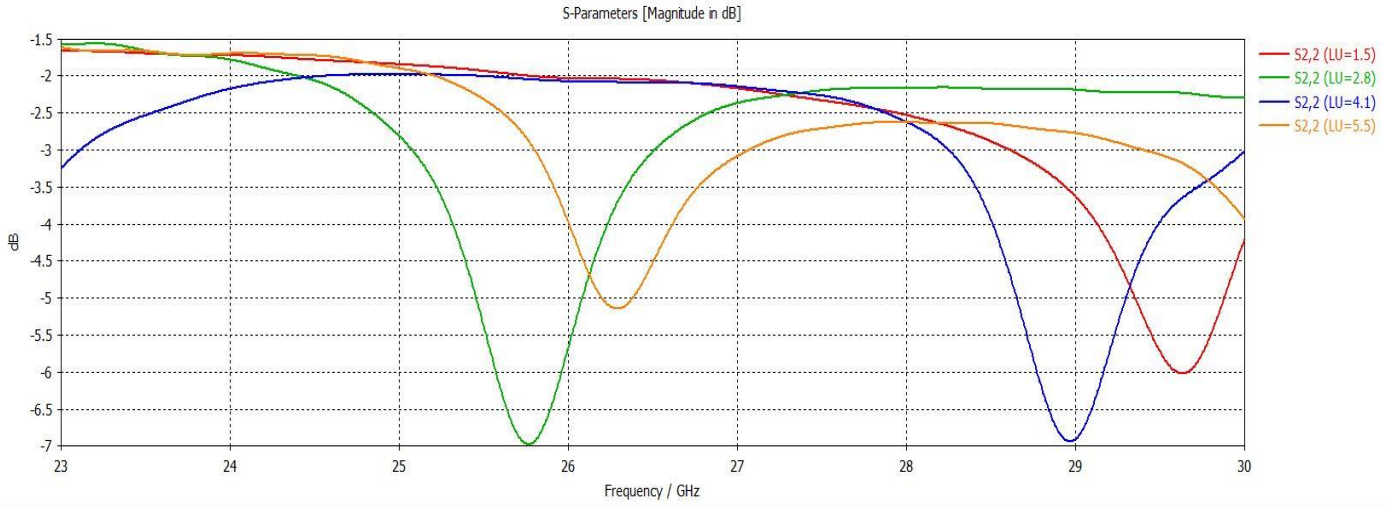


Figure 24. Varying patch length (LU_p) of the 5G band array

The same variations can be observed from the above figure for the 5G band array as like the DSRC band array.

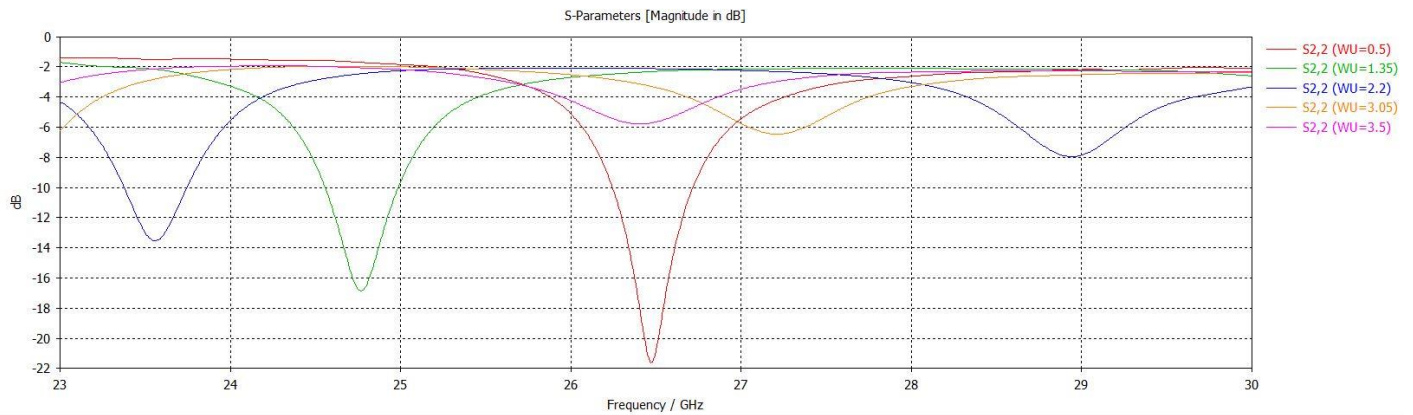


Figure 25. Varying patch width (WU_p) of the 5G band array

Besides the length and width of the antenna, height of the substrate also causes frequency shift. Thicker substrate shifts the frequency more towards higher frequency range. It can be depicted in the below figures.

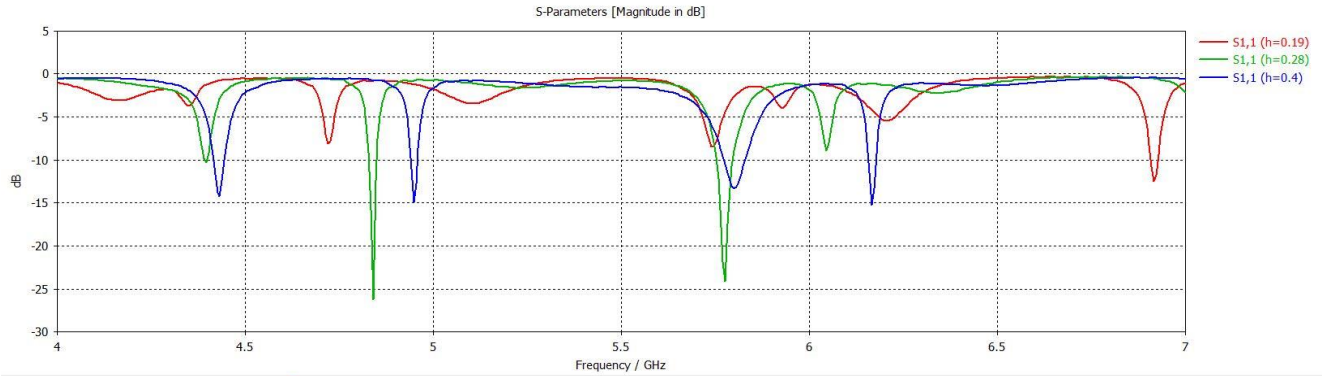


Figure 26. Varying thickness of the substrate EPOCH 1

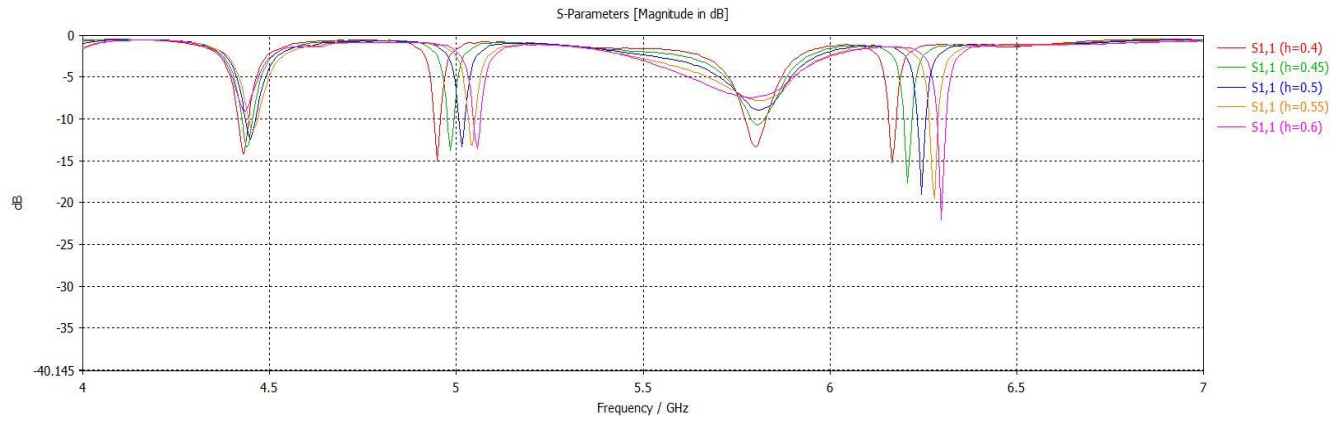


Figure 27. Varying thickness of the substrate EPOCH 2

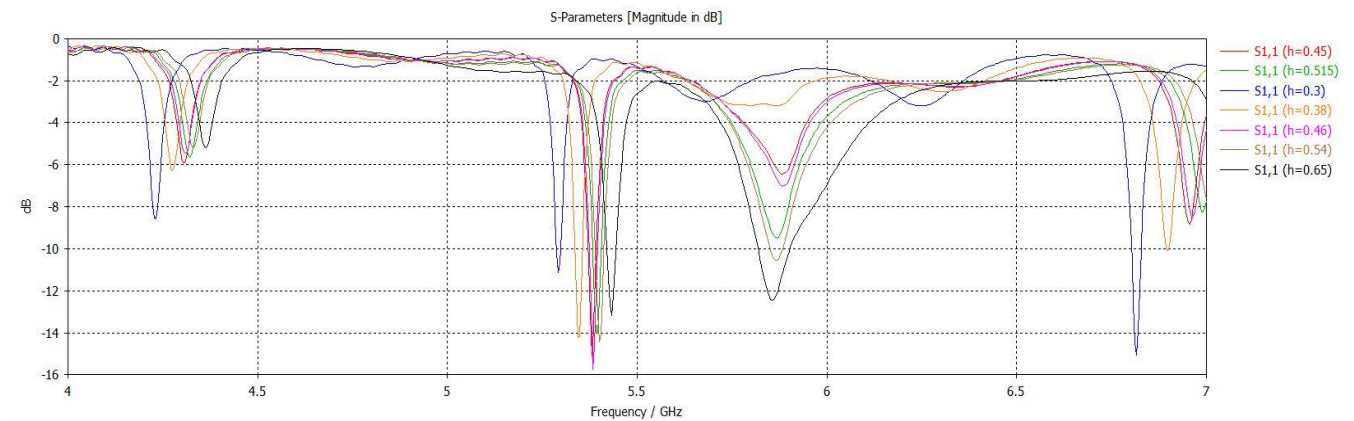


Figure 28. Varying thickness of the substrate EPOCH 3

SIMULATION RESULTS:

S PARAMETERS:

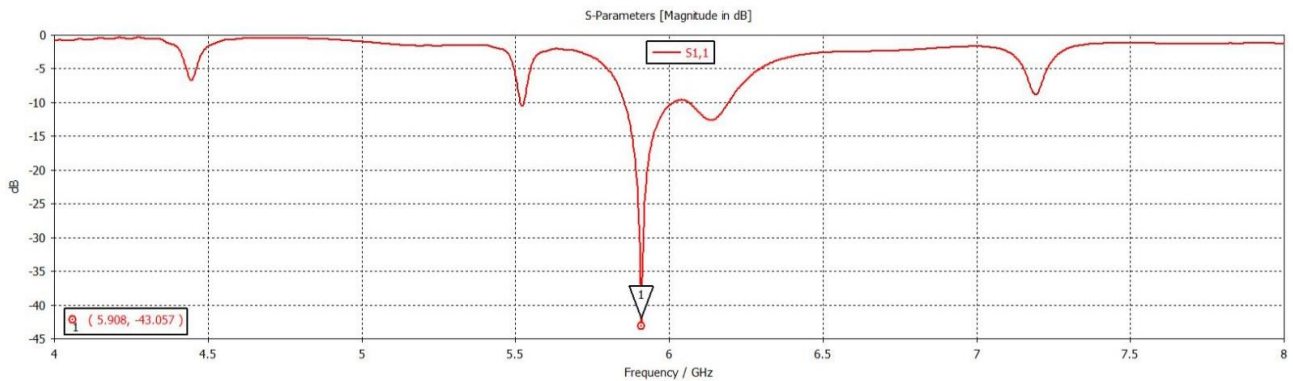


Figure 29. S11 Plot after slot introduction

Comparing to the previous Rogers design, less S11 (return loss) is observed (-43.057 dB).

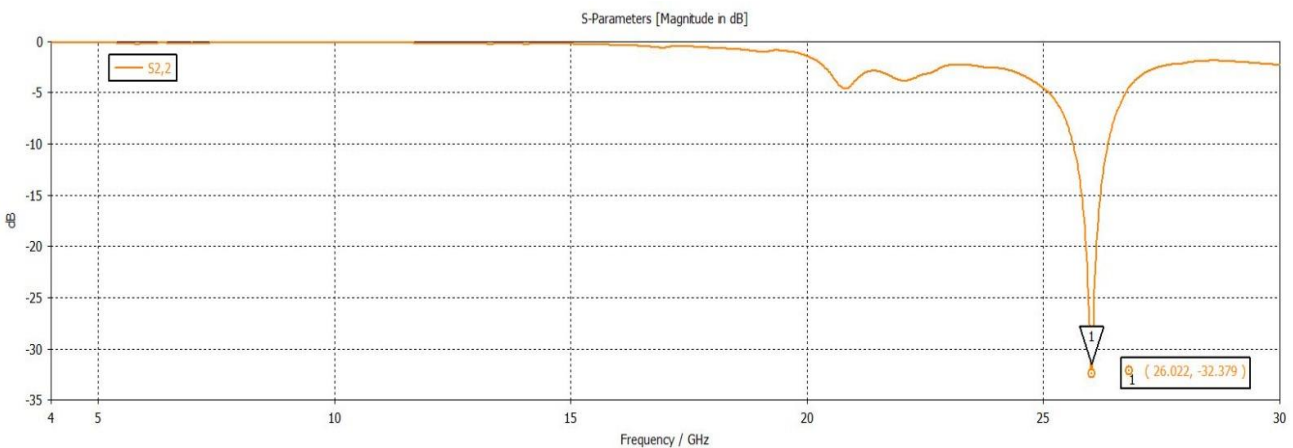


Figure 30. S22 Plot after slot introduction

As 28 GHz is a 5G mm wave band used in the countries like US, Canada, South Korea and Japan. 26 GHz is the 5G mm wave band allocated for India. Hence the Upper band array for 5G applications has been shifted to 26 GHz. Also an acceptable dip in the S parameter has been achieved at this frequency (-32.379 dB).

RADIATION PATTERN:

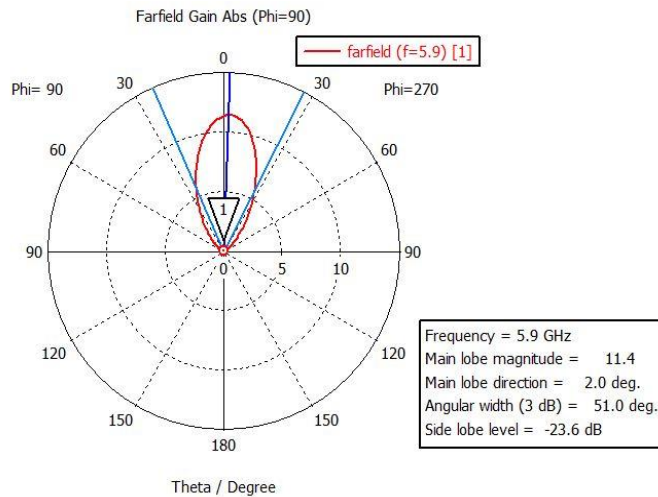


Figure 31. Radiation pattern of shared array at 5.9 GHz – Rogers based design

Table 11.

Simulation results for 5.9 GHz array
-Rogers based design

Parameter	Value
Gain	10.5 dB
Directivity	11.1 dB
Efficiency	86.6%
HPBW	54.5°
VSWR	1.36

Table 12.

Simulation results for 26 GHz array
-Rogers based design

Parameter	Value
Gain	9.778 dB
Directivity	9.974 dB
Efficiency	95.6%
HPBW	43.9°
VSWR	1.03

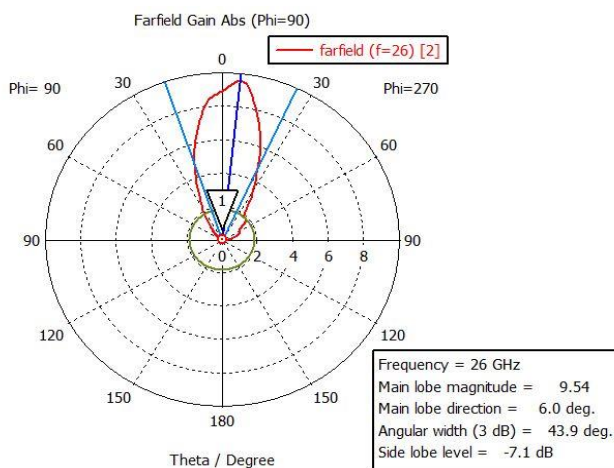


Figure 32. Radiation pattern of shared array at 26 GHz – Rogers based design

The figure shows that due to the introduction of cross slots in the previous Rogers design, the minor lobe found in the radiation pattern of that design got eliminated and as a result, the efficiency of the modified Rogers design has been increased.

VSWR PLOTS:

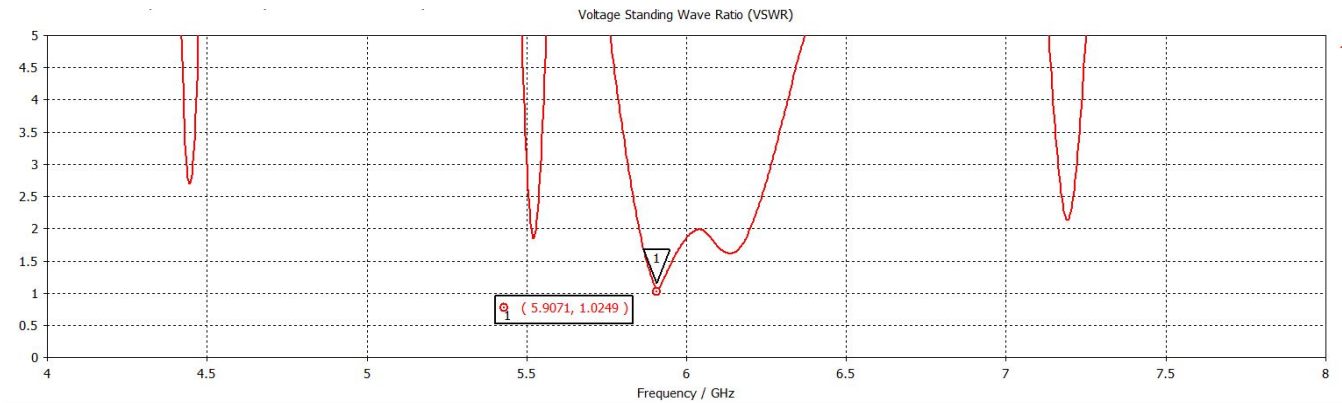


Figure 33. VSWR at 5.9 GHz – Rogers based design

The smaller the VSWR is, the better the antenna is matched to the transmission line and the more power is delivered to the antenna. The minimum VSWR is 1.0. From the above figure, at DSRC band, the VSWR has measured to be 1.0249 which is very much nearer to the ideal value indicating that the reflected power is a near zero value.

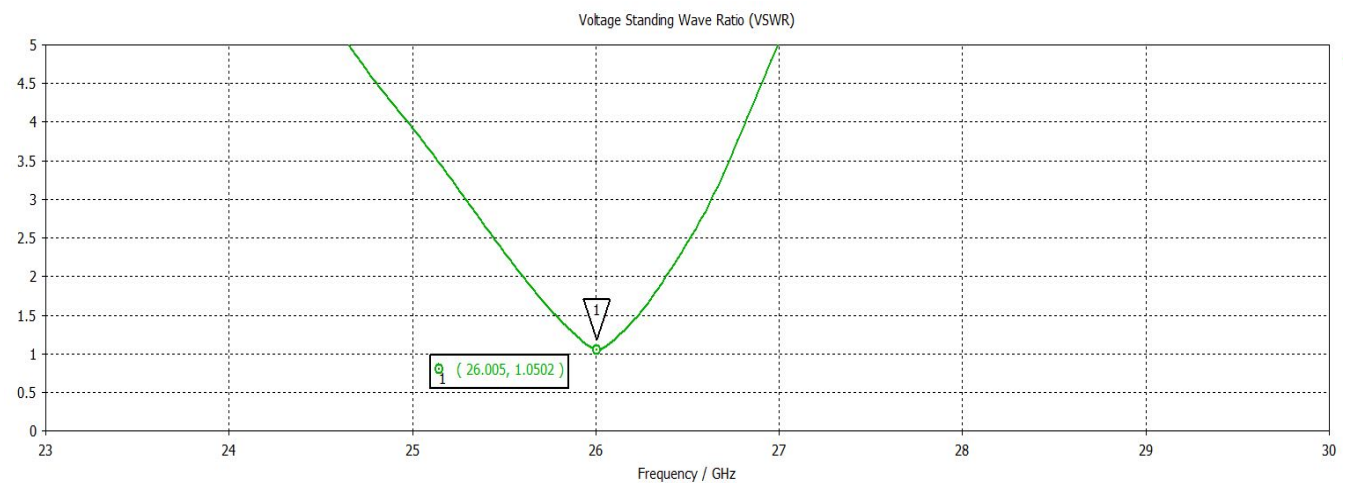


Figure 34. VSWR at 26 GHz – Rogers based design

Also, at 5G band, the VSWR has measured to be 1.0502 indicating that the reflected power is a near zero value (almost no reflected power).

AXIAL RATIO:

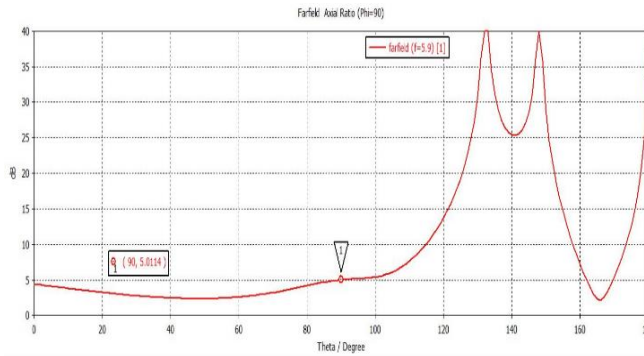


Figure 35. Axial ratio at DSRC band– Rogers based design

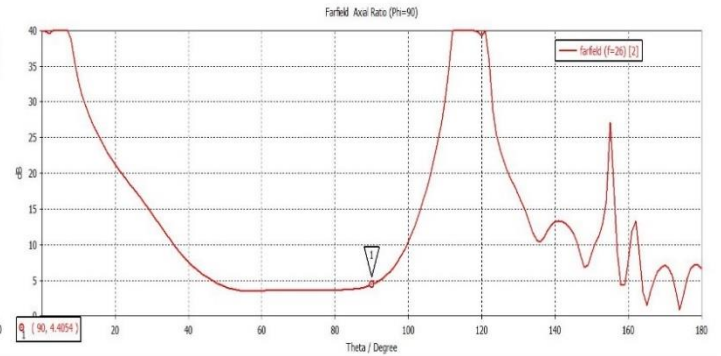


Figure 36. Axial ratio at 5G mm-wave band– Rogers based design

Axial ratios are often quoted for antennas in which the desired polarization is circular. The ideal value of the axial ratio for circularly polarized fields is 0 dB. The axial ratio for an ellipse is larger than 1 (> 0 dB) and less than 3 dB. The axial ratio for pure linear polarization is infinite, because the orthogonal components of the field is zero. Referring to the above diagrams, at both DSRC and 5G band axial ratio appears to be in the range of 5.0 dB at DSRC band and 4.4 dB at 5G band. Hence, the modified Rogers design has the properties of **Elliptical polarization**.

3.6 ANALYSIS IV:

FR4 DESIGN SIMULATION RESULTS:

- Owing to the evolution of vehicular communication, it is important to reduce the overall design cost of the system by choosing cost-efficient materials for the design.
- Since the cost of Rogers substrate is very high, FR4 substrate has been chosen for design consideration which is a low-cost material.
- Hence, the design has been modified with material from Rogers to FR4 and expected results have been achieved.

S-PARAMETERS:

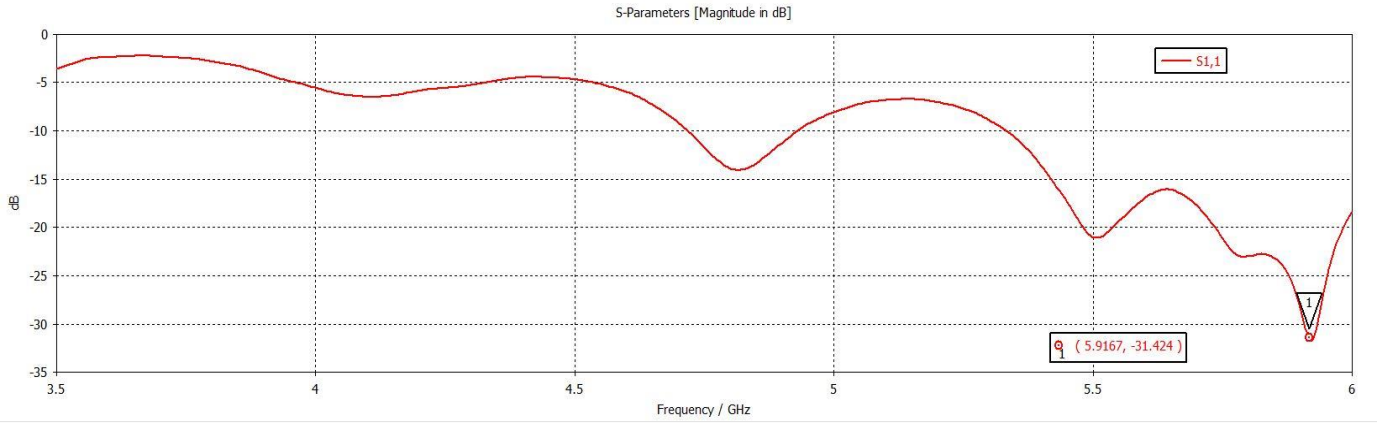


Figure 37. S₁₁ Plot for 5.9 GHz array – FR4 based design

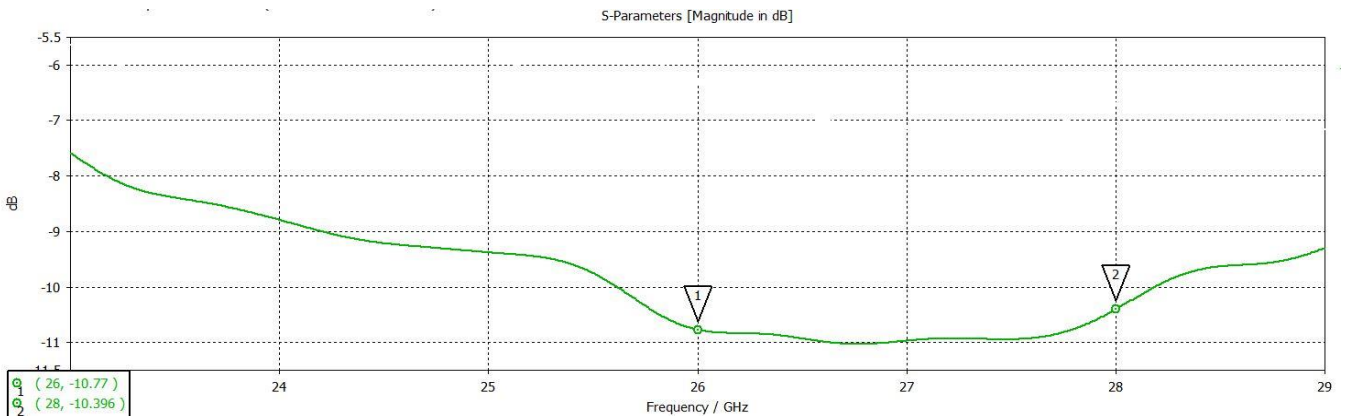


Figure 38. S₂₂ Plot for 5G mm-wave band – FR4 based design

From the above figure, during the excitation of both DSRC band array and 5G band array, it has been observed that the S₁₁ has a considerable dip of about -31.424 dB and S₂₂ with a dip of -10.77 dB at 26 GHz and -10.396 dB at 28 GHz. Hence at 5G band, a much wider bandwidth (greater than 2 GHz) is achieved.

RADIATION PATTERN:

Different antenna designs produce different radiation patterns. The complexity of the pattern depends on the antenna's design and construction. Antenna specification sheets sometimes come with three-dimensional projections. More often, a two-dimensional plot can be observed and visual representation of Radiation pattern in three-dimensional pattern gives us more information.

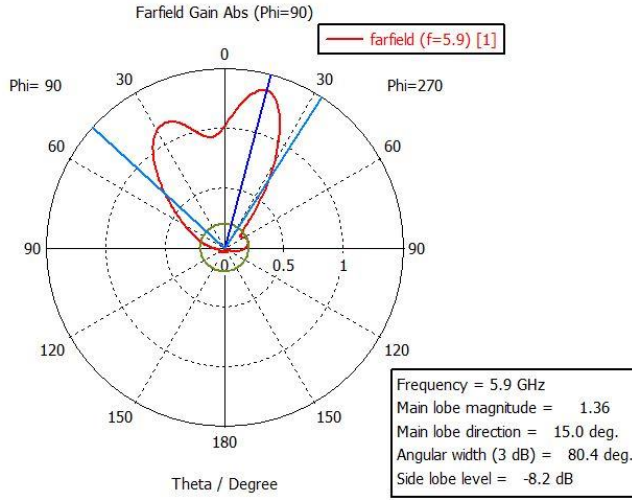


Figure 39. Radiation pattern of shared array at 5.9 GHz – FR4 based design

Table 13. Simulation results for 5.9 GHz array – FR4 based design

Parameter	Value
Gain	6.87 dB
Directivity	8.138 dB
Efficiency	64.82%
HPBW	80.4°
VSWR	1.0801

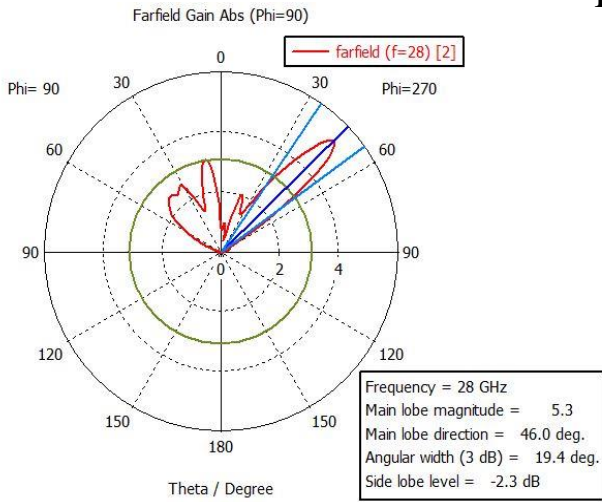


Figure 40. Radiation pattern of shared array at 5G mm-wave band – FR4 based design

Table 14. Simulation results for 5G mm-wave band – FR4 based design

Parameter	Value
Gain	7.201 dB
Directivity	9.188 dB
Efficiency	63.21%
HPBW	19.4°
VSWR	1.8658

The obtained results are as expected and supports V2V communication and 5G mm-wave band. But still parameters like efficiency and radiation pattern are better in the antenna array made up of Rogers substrate. FR4 is popularly known for its cost efficiency and is used worldwide.

VSWR PLOTS:

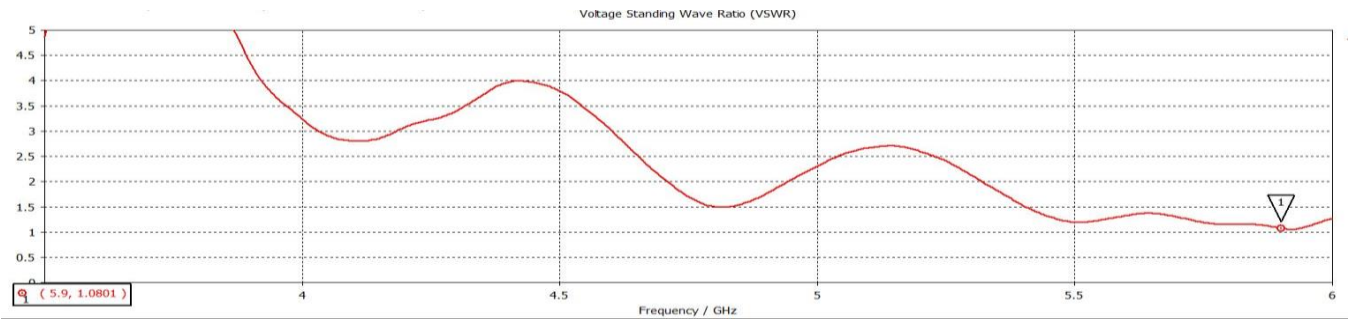


Figure 41. VSWR at 5.9 GHz – FR4 based design

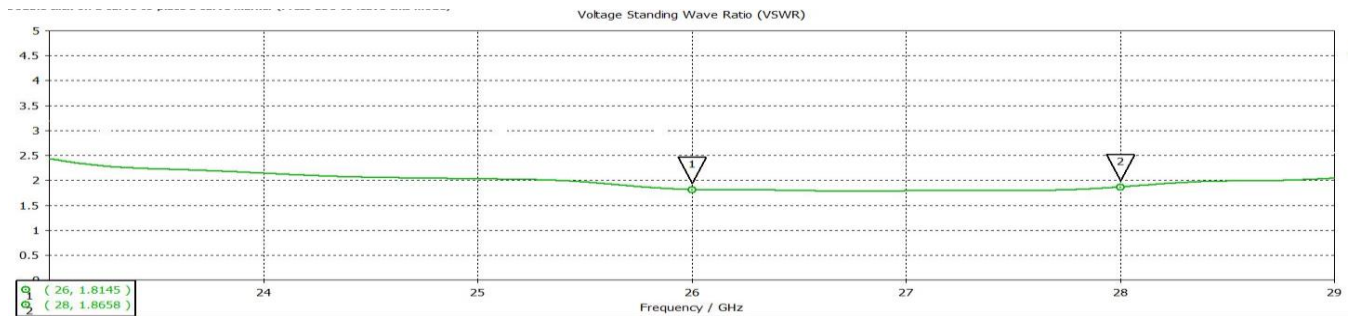


Figure 42. VSWR at 5G Band – FR4 based design

Referring to the ideal values of VSWR, it has been observed that at DSRC band an acceptable VSWR of 1.081 and at 5G band also a moderate VSWR of about 1.8658 has been achieved.

AXIAL RATIO:

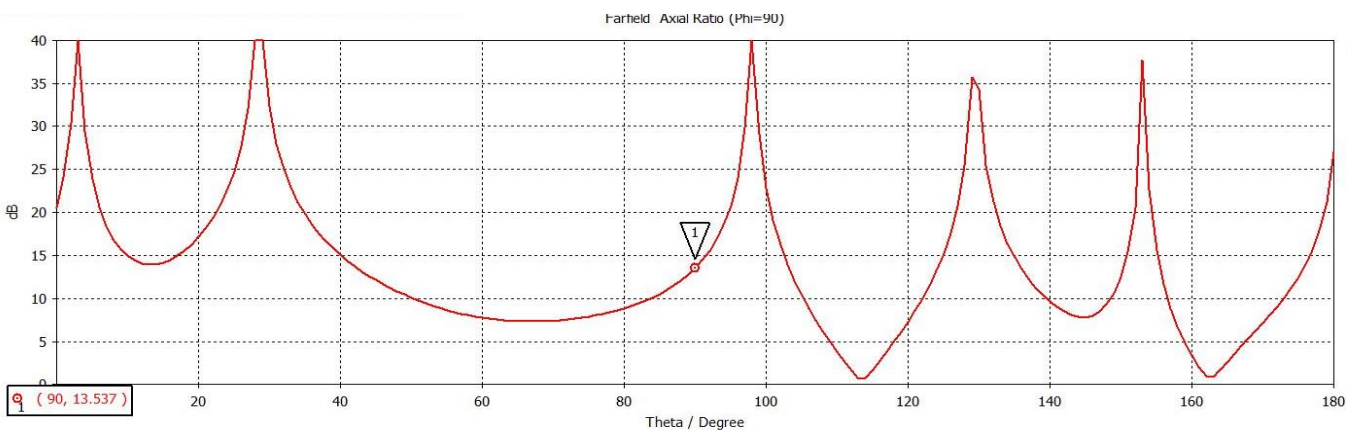


Figure 43. Axial ratio at 5.9 GHz – FR4 based design

Referring to the above figure, as the axial ratio occurs in the range of 13.557 dB, the antenna designed using FR4 substrate has the properties of linear polarization.

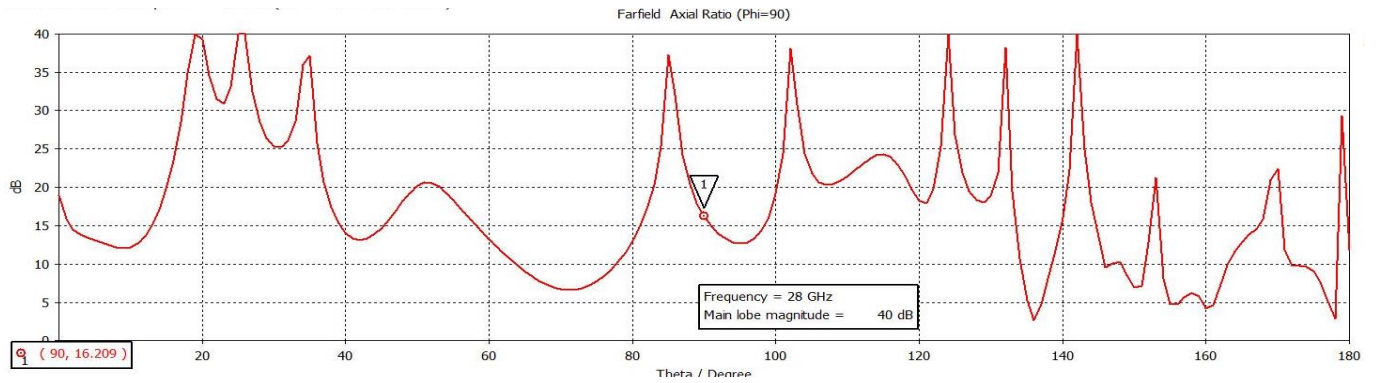


Figure 44. Axial ratio at 5G mm-wave band – FR4 based design

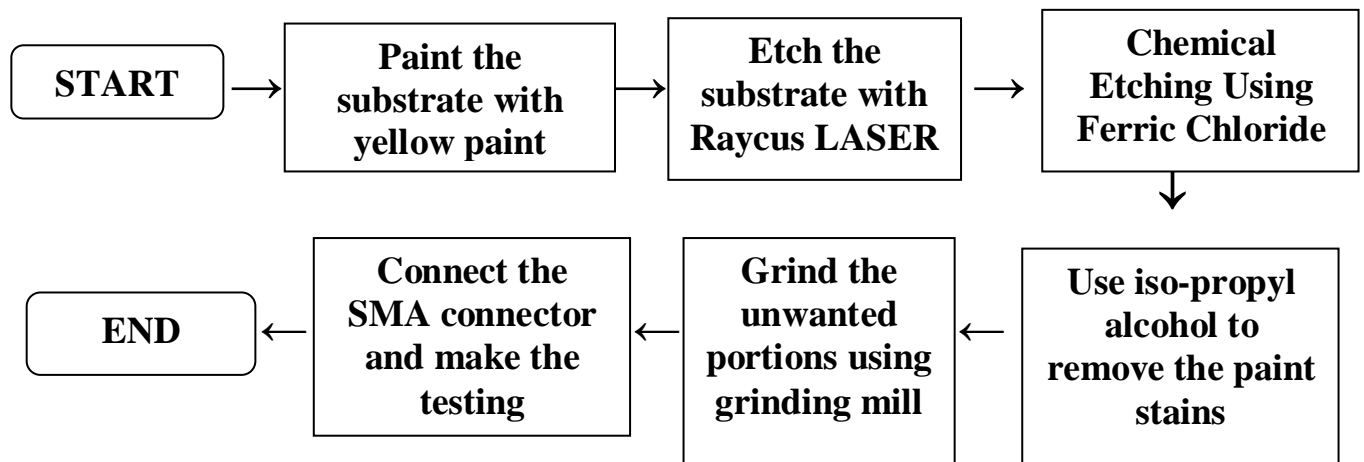
From the above figure, it has been observed that the axial ratio at 5G mm-wave band is 16.209 dB, stating that port 2 of the FR4 designed antenna operating at 5G mm-wave band has the properties of linear polarization.

CHAPTER 4

FABRICATION PROCESS

4.1 LASER CUM CHEMICAL ETCHING

This chapter discusses the various techniques used for antenna fabrication. The antennas fabricated using different techniques were then compared for their performance, to identify the most suitable fabrication methodology.



4.1.1 LASER ENGRAVING:

Laser engraving is a process that vaporizes materials into fumes to engrave permanent, deep marks. The laser beam acts as a chisel, incising marks by removing layers from the surface of the material. The laser hits localized areas with massive levels of energy to generate the high heat required for vaporization. Laser engraving sublimates the material surface to create deep crevices. This means that the surface instantly absorbs enough energy to change from solid to gas without ever becoming a liquid. To achieve sublimation, the laser engraving system must generate enough energy to allow the material's surface to reach its vaporization temperature within milliseconds.



Figure 45. RAYCUS LASER



Figure 46. IPG LASER

Using the EZCAD software, the image is imported. X and Y coordinates of the design are given as inputs from which many passes are run to etch the design.

4.1.2 CHEMICAL ETCHING:

The chemical etching process works by printing a component design on to photo resist which is laminated onto metal. The areas of photo resist which have not been printed are removed, exposing the metal, which is subsequently etched away. Chemical etching, also known as chemical milling or photo etching, is a subtractive sheet metal machining process which uses chemical etchants to create complex and highly accurate precision components from almost any metal. Photo-etched components are burr and stress-free with no mechanical force or heat used, leaving material properties unaltered. Ferric chloride is one of the most widely used etchants in the field of chemical etching. It is commonly used to etch steel and stainless steel parts, but it is also capable of etching copper. One of the reasons it is so popular is because of its versatility.



Here the Copper of the substrate reacts with the Ferric Chloride and dissolve in the solution as CuCl_2 . In a solution the Ferric chloride and distilled water are mixed in 1:1 ratio to get the perfect etching of the copper.

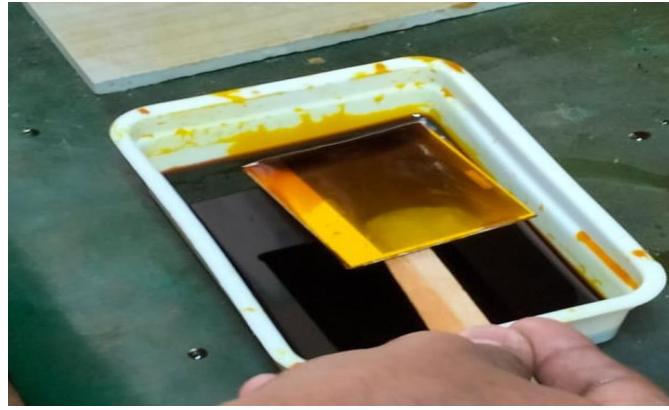


Figure 47. After reaction with FeCl_3

4.2 FINAL PREPARATIONS:

After the chemical etching of the laser fabricated material the paint stains in the material is removed using the Isopropyl alcohol. Isopropyl alcohol (rubbing alcohol) liquefies the oldest paint. Wet paint thoroughly and cover with plastic to prevent evaporation. Paint will wash off with water after a short time.

4.2.1 PHOTO POLYMERIZATION:

A negative acting photo polymerizable film resist in which a photopolymerizable layer is sandwiched between a temporary support film and a temporary cover film. This film has gained widespread usage in the manufacture of printed circuits in which the cover film is removed, the photopolymerizable layer is laminated by heat and pressure to the surface, e.g., copper, of a substrate to be permanently modified, the layer is image wise exposed to actinic radiation, the film support is removed, the unexposed areas of the layer are removed by solvent washout (development), and the resultant bared area of the copper surface is permanently modified, such as by etching or deposition of metal.

4.2.2 TINNING:

Tinned copper is primarily used for protection against oxidation and corrosion. In climates where copper has long-term exposure to water, the oxygen will combine with the

metal and form copper oxide, weakening the bonds of the metal. It is worse if the wire is in contact with salt water.



Figure 48. During tinning process

4.2.3 GRINDING:

Finally the fabricated antenna is grinded using the grinding machine .Grinding machine grinds the unwanted area in the antenna. Grinding is used to avoid unnecessary losses in the substrate while cutting the antenna.



Figure 49. During Grinding process

4.3 LASER DEPANELING:

LASER Depaneling is one of the most modern and promising processes for separation PCBs from the overall panel. During the depaneling process, the previously manufactured and assembled printed circuit boards (PCBs) are cut out of the panel using a suitable separation process/tool. In the case of laser depaneling, the singulation process is performed by a focused laser beam that ablates the material layer by layer. LPKF machine (Leiterplatten Kopierfrasen – Circuit Board Copy Milling) is used for this

purpose. The LPKF lasers are suitable for cutting all industry-standard panel sizes with dimensions of up to 533 x 610 mm (2" x 2"). The 20- μ m high-quality UV laser kerf width allows for cutting of even the most delicate contours at high speeds. The following steps give a detailed explanation about the step-by-step procedure involved in the fabrication process.



Figure 50. LPKF Machine

4.3.1 STEP 1: EXPORTING THE GERBER FILES:

First step is to export the Gerber files of each layer of the antenna to be fabricated.

- Open CST simulation
- Use pick faces and select the layer
- Align coordinates with WCS.
- Click modelling and select Export GERBER.
- Choose GERBER single layer.

4.3.2 STEP 2: IMPORTING THE GERBER FILES:

Gerber files are imported into the CIRCUIPRO software. Appropriate calibrations

are made to have proper etching of the patch.

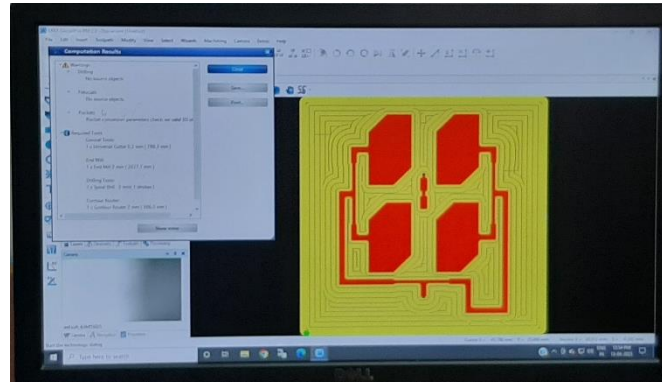


Figure 51. Gerber of the array

4.3.3 STEP 3: INSERTION OF APPROPRIATE DRILL BEATS:

After importing the Gerber file of the array, drill beats should be chosen such that accurate etching of the layer is made and holes of proper diameter are made as per the simulation design.

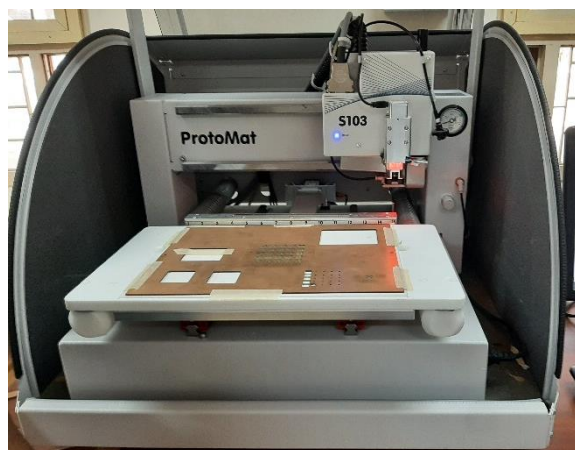


Figure 52. Insertion of drills beats

4.3.4 STEP 4: ETCHING OF THE SUBSTRATE:

After STEP 3, many passes have to be made to have perfect etching of the substrate without any unwanted copper layers. If proper etching is not achieved even after many iterations, then chemical etching has to be done.

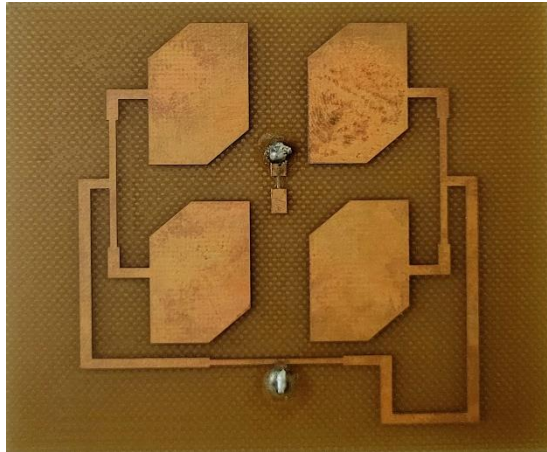


Figure 53. Etched Substrate

4.3.5 STEP 5: SOLDERING OF PORTS:

After the antenna has been etched perfectly, holes are drilled using 1mm drill bit. Two ports have been inserted and soldered SMA connector with ground plane.

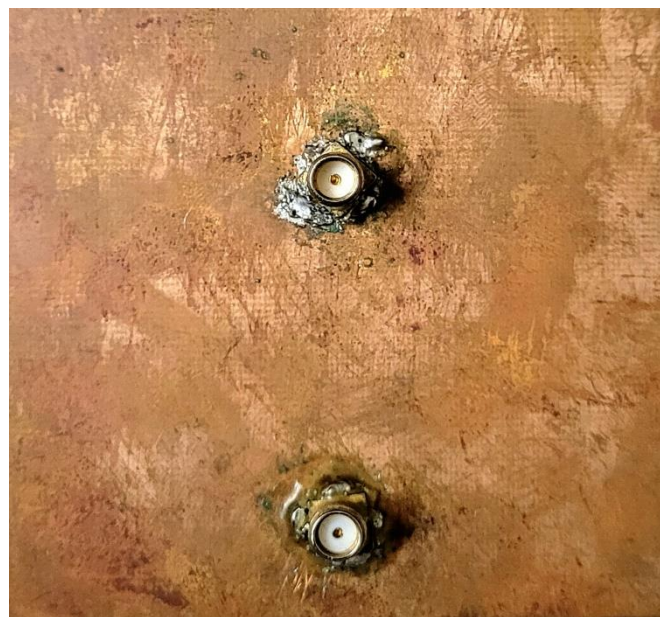


Figure 54. Soldered ports

4.4 NETWORK ANALYSER:

A network analyzer is an instrument that measures the network parameters of electrical networks. Today, network analyzers commonly measure S parameters because reflection and transmission of electrical networks are easy to measure at high frequencies,

but there are other network parameter sets such as y-parameters, z-parameters, and h-parameters. Network analyzers are often used to characterize two-port networks such as amplifiers and filters, but they can be used on networks with an arbitrary number of ports. A VNA (Vector Network analyzer) is a form of RF network analyzer widely used for RF design applications. A VNA may also be called a gain–phase meter or an automatic network analyzer.

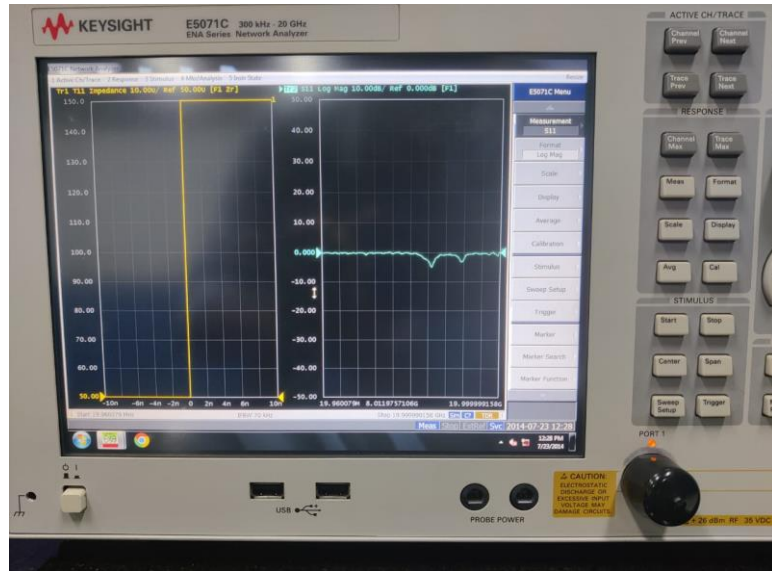


Figure 55. Vector Network Analyzer

4.5 CALIBRATION KIT:

Calibration kit is used to remove the noise which were present in the previous simulation. It contains three port namely OPEN, SHORT, LOAD .These three ports were connected to the measuring tube and the noises where removed. CALKIT 85220A is used for testing.



Figure 56. Calkit 85220A

4.6 SMA CONNECTOR:

SMA (*SubMiniature version A*) connectors are semi-precision coaxial RF connectors developed in the 1960s as a minimal connector interface for coaxial cable with a screw-type coupling mechanism. The connector has a $50\ \Omega$ impedance. SMA was originally designed for use from DC (0 Hz) to 12 GHz, however this has been extended over time and variants are available to 18 GHz and 26.5 GHz. There are also mechanically compatible connectors such as the K-connector which operate up to 40 GHz. The SMA connector is most commonly used in microwave systems, hand-held radio and mobile telephone antennas and, more recently, with WiFi antenna systems and USB software-defined radio dongles. It is also commonly used in radio astronomy, particularly at higher frequencies (5 GHz+).



Figure 57. SMA Connector

CHAPTER 5

FABRICATION RESULTS

5.1 RESULTS:

5.1.1 RETURN LOSS OF DSRC BAND:

The fabricated antenna using FR4 substrate is tested and analysis were made using Vector network Analyzer. Following Figure shows the S11 of the fabricated antenna. The Fabricated antenna has good return loss of -20 decibel.



Figure 58. Measured S11 of DSRC band

5.1.2 VSWR AT DSRC BAND:

VSWR (Voltage Standing Wave Ratio) is a measure of how efficiently radio-frequency power is transmitted from a power source, through a transmission line, into a load. In an ideal system, 100% of the energy is transmitted. This requires an exact match between the source impedance, the characteristic impedance of

the transmission line and all its connectors, and the load's impedance. The signal's AC voltage will be the same from end to end since it runs through without interference.

The following plot shows the VSWR at DSRC band. The Ideal value of VSWR should lie in the range of 1 to 2. The fabricated antenna has good VSWR of 1.02 at DSRC band.

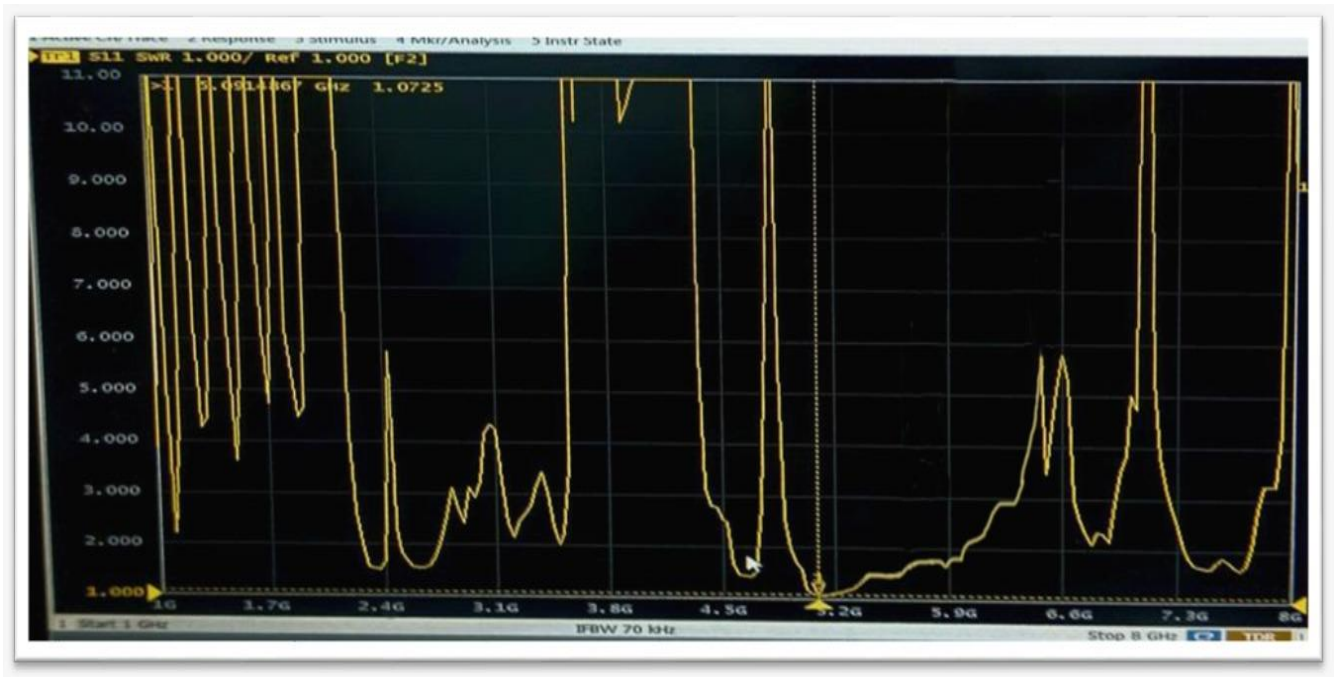


Figure 59. Measured VSWR at DSRC band

CHAPTER 6

CONCLUSION

In this Project, a Low Profile Dual band shared antenna array has been simulated and fabricated for Vehicle to Vehicle communication (DSRC band) and 5G mm-wave band for which the proper isolation between the two ports for DSRC band and 5G mm-wave band has been achieved by providing differential feed to the patch array operating at 5.9 GHz and co-printing a series fed array operating at 5G band on the same substrate in the space within the 5.9 GHz array. Through several iterations and parametric analysis, the effects of introducing cross slots, truncated corners, varying length and width of patch and varying thickness of the substrate were studied and as a result, the dimensions have been reduced from $100 \times 75 \text{ mm}^2$ to $75 \times 75 \text{ mm}^2$ for both the antenna arrays made up of Rogers and FR4 substrates and truncated corners have been introduced in FR4 based design and cross slots cum truncated corners of appropriate dimensions have been introduced in the Rogers based design to get better results in terms of radiation pattern, efficiency, gain and polarization. The antenna designed using Rogers substrate supports DSRC band at 5.9 GHz with a gain of 10.63 dB and efficiency of 85.41% and 5G mm-wave band at 26 GHz with a gain of 9.78 dB and efficiency of 95.6%. The antenna designed using FR4 substrate supports DSRC band at 5.9 GHz with a gain of 6.87 dB and efficiency of 64.82% and 5G mm-wave band at 28 GHz with a gain of 7.2 dB and efficiency of 63.21%. From experimental results, the S11 parameters and VSWR plots are reported and it is concluded that the suggested design can be used for mentioned applications.

REFERENCES

1. Sandhiya Reddy Govindarajulu , Rimon Hokayem , M D Nurul Anwar Tarek , Marisol Roman Guerra Elias A. Alwan (October 2021) “Low Profile Dual-Band Shared Aperture Array for Vehicle-to-Vehicle Communication”.
2. Deven G. Patanvariya, Kalyan S. Kola, Anirban Chatterjee (April 2019) “Left-Handed Circularly Polarized Two-Element Antenna Array for Vehicular Communication”.
3. Adamantia Chletsou, John F Locke, John Papapolymerou (November 2021) “Vehicle Platform Effects on Performance of Flexible, Lightweight and Dual-Band Antenna for Vehicular Communications”.
4. Edith Condo Neira , Jan Carlsson , Kristian Karlsson , Erik G Strom (October 2006) “Combined LTE and IEEE 802.11p Antenna for Vehicular Applications”.
5. Huapeng Zhao, Xinhui Zhang, Zhizhang Chen, Ying-Chang Liang (May 2021) “A Hybrid-Equivalent Surface-Edge Current Model for Simulation of V2X Communication Antennas With Arbitrarily Shaped Contour”.
6. Yuanxi Cao, Sen Yan, Jianxing Li, Juan Chen (July 2022) “A Pillbox Based Dual Circularly-Polarized Millimeter-Wave Multi-Beam Antenna for Future Vehicular Radar Applications”.
7. Ani Taggu, Bikram Patir, Utpal Bhattacharjee (March 2017) “A dual band omnidirectional antenna for WAVE and Wi-Fi”.
8. Shobit Agarwal, Ashwani Sharma (November 2020) “A Miniaturized Wideband Antenna for Vehicular Communication, WiMAX, and WLAN Applications”.